UCBNE-5101

Effective Application
of
Partitioning and Transmutation Technologies
to
Geologic Disposal

Report Submitted to Japan Atomic Energy Agency (JAEA)
for Collaborative Research Between Department of Nuclear Engineering, University of California, Berkeley, and Japan Atomic Energy Agency for FY2005

by

Joonhong Ahn
Department of Nuclear Engineering
University of California, Berkeley

January 2006

Comments and notification of any errors

in this report would be appreciated.

Joonhong Ahn
Department of Nuclear Engineering
University of California
Berkeley, CA 94720
USA

ahn@nuc.berkeley.edu

Table of Contents

I. Executive Summary for Project 1
I.1 Background 1
I.1.1 Achievements in FY2003 1
I.1.2 Achievements in FY2004 1
I.2 Statement of Work for FY2005 2
I.3 Summary of Results and Conclusions from Project in FY2005 2
I.4 Recommendations for Future Works 3
II. Introduction 4
III. Environmental Impact 6
III.1 Environmental Impact Measure 6
III.2 Radionuclide Transport in Repository 7
III.3 Formulae for Peak mass Factor P 8
IV. Waste Conditioning Model 12
IV.1 Linear-Programming Problem 12
IV.2 Constraints 13
V. Numerical Results and Discussions 16
V.1 Waste Conditioning for PWR Spent Fuel Reprocessing 16
V.2 Waste Conditioning for FBR Spent Fuel Reprocessing 21
V.3 Mass Loadings of Selected Radionuclides in HLW Canister 27
V.4 Parameter Values for Radionuclide Release and Transport 29
V.5 Results for Environmental Impact Evaluation 31
V.6 Effects of Mass Loading in HLW Canister on Environmental Impact 33
V.7 Bounding Analysis for Uncertainty with Transport Parameters 34
V.8 Advantages of FBR 38
VI. CONCLUSIONS 40
VII. REFERENCES 42
Appendix: Input Data Files for ORIGEN2 Calculations 43
FBR Core Fuel 43
FBR Axial Blanket Fuel 43
FBR Radial Blanket Fuel 44

List of Figures

Figure 1: A two-dimensional array configuration of a geologic repository. There are N_y rows, each containing N_x waste canisters in the water-flow direction. The numbers N_x and N_y do not have to be the same as actual repository configuration. The number N_x should be determined by considering hydrological connection among canisters. Thus, a repository would consist of many rows with different N_x. The number N_y then should be determined to match the total number of canisters, i.e., total number of canisters = $\sum_{j=1}^{N_y} N_{x,j}$. In this study, however, all the rows consist of the same number N_x of hydrologically connected canisters. 8

Figure 2: Conceptual diagram for optimization of waste loading in HLW solidification. 12

Figure 3: Linear approximation for the filled waste volume constraint 14

Figure 4: Graphical solution for optimum PWR-HLW conditioning 20

Figure 5: Graphical solution for optimum FBR-HLW conditioning 27

Figure 6 : Environmental impact from a repository containing 40,000 canisters as a function of the number of canisters connected in the same water flow stream. The left and right figures show the cases for LWR and FBR, respectively. The solid curves represent actinide radionuclides, whereas the dashed curves FP radionuclides. 32

Figure 7: Effects of reduction in initial mass loadings per canister on the environmental impact from a 40,000-canister repository due to ^{237}Np, ^{242}Pu ^{240}Pu, and ^{239}Pu. Nx = 1 is assumed. For each curve, the mass loadings shown in Table VI for the PWR and FBR cases are indicated by arrows. 33

Figure 8: Effects of non-dimensionalized parameters on environmental impact of ^{237}Np and ^{240}Pu. Long-lived FP shows similar tendency as ^{237}Np. For ^{240}Pu, the lower bound curve is far below. The arrows close to the left axis show the uncertainty ranges for the environmental impact. 36

List of Tables

Table I: Formulae for Peak Mass Factor P for Congruent Release 9
Table II: Formulae for Peak Mass Factor P for Solubility-Limited Release 11
Table III: HLW Composition Vector and Decay Heat Calculation for HLW from 1 Metric Ton of PWR Spent Fuel 17
Table IV: Composition of the Glass Frit, PF798, Developed by JNC [9] 19
Table V: HLW Composition Vector and Decay Heat Calculation for 1500 MWe FBR Operation 23
Table VI: Mass Loadings of Important Radionuclides in a Canister of Solidified HLW and Their Parameter Values for Environmental Impact Evaluations. 28
Table VII: Values of Transport Parameter Assumed for Environmental Impact Assessment, Based on H-12 Repository Design 30
Table VIII: Values for Geochemical Parameters for Environmental Impact Assessment, Based on Those Assumed for H-12 Repository Performance Assessment [8] 30
Table IX: Values of Non-Dimensionalized Parameters for Radionuclides Released Under Solubility-Limited Release Mode 30
Table X: Values of Non-Dimensionalized Parameters for Congruently-Released Radionuclides 31
Table XI: Uncertainty Ranges for Solubility Limited Radionuclides for $N_x = 1$. 35
Table XII: Ranges of Environmental Impact for Solubility-Limited Nuclides Resulting From Uncertainties Associated with Non-Dimensionalized Parameters 35
Table XIII： Uncertainty Ranges for Congruent-Release Radionuclides for $N_x = 1$. 37
Table XIV: Ranges of Environmental Impact for Congruent-Release Nuclides Resulting From Uncertainties Associated with Non-Dimensionalized Parameters 37

I. Executive Summary for Project

I.1 Background

The cooperative study between Japan Nuclear Cycle Development Institute[1] (JNC hereafter) and the Department of Nuclear Engineering, University of California, Berkeley (UCBNE hereafter), titled "Research on Effective Application of Partitioning and Transmutation Technologies to Geologic Disposal," has been carried out for the past two years.

I.1.1 Achievements in FY2003

The waste-conditioning model based on the waste stream from the advanced reprocessing process being developed at JNC was established by applying a linear-programming approach. Analyses were made for the environmental impact for LWR-recycle and the base FBR-recycle cases with or without P/T. Environmental impacts from base-case scenarios were quantitatively evaluated.

The results show that environmental impact of vitrified HLW disposed of in an H12-type repository would be significantly smaller than that from the direct disposal of commercial spent fuel from LWRs on the GWyr basis. In the case of vitrified HLW, by observing the release rates from the repository, major impact contributors are found to be Np-237 and Cs-135. Because environmental impact of Cs-135 is about a factor of 10 smaller than that from Np-237, partitioning 90% of Np and its decay precursors from the HLW would reduce environmental impact effectively.

I.1.2 Achievements in FY2004

Based on the mathematical formulations for the radionuclide release rate from the repository region, developed in FY2003, the formulas for the peak mass of a radionuclide in the environment were derived. The peak mass of a radionuclide is expressed in terms of the canister-array configuration in a repository, the initial mass loading of the radionuclide in the waste canister, and the engineered-barrier parameters. The peak mass can be converted to the peak environmental impact of the repository.

Utilizing the peak-mass formulas (developed in FY2004) and the waste-conditioning

[1] Japan Atomic Energy Agency since October 1, 2005.

model (developed in FY2003), the relationship between environmental impact and the system parameters (the fuel cycle, the waste conditioning and the repository design) was investigated.

It was shown that HLW from the FBR with minor actinide recycle results in significantly smaller environmental impact for the same electricity generation. Quantitative relationship between the separation efficiency of minor actinides and the environmental impact was also obtained, which could be utilized to set a technological target for separation process design.

A paper was presented at "Actinide and Fission Product Partitioning & Transmutation," Eighth Information Exchange Meeting, Las Vegas, Nevada, USA, 9-11 November 2004, OECD/NEA.

I.2 Statement of Work for FY2005

Based on these achievements, the following are proposed as tasks for FY2005:

- Apply the waste conditioning model to the FBR fuel cycle, and investigate the effects of recycle parameters on the waste compositions and the number of waste canisters per unit electricity generation, and on the environmental impact of HLW disposed of in a geologic repository. Based on the results, develop a scheme for the repository capacity expansion.
- Based on the current knowledge about uncertainties associated with repository parameters, perform uncertainty analyses to quantify the uncertainty with the environmental impact of the repository for various fuel cycle schemes.
- Start the model expansion to include the contributions of TRU wastes, and make a preliminary comparative study for the effects of TRU wastes on the environmental impact of a fuel cycle.

I.3 Summary of Results and Conclusions from Project in FY2005

- In the HLW from PWR spent fuel, ^{237}Np including its decay precursors are the major sources of environmental impact.
- The environmental impact from a FBR-HLW repository is smaller than that from the FBR repository by a factor of 10. If compared on a per GWyr basis, the advantage of FBR is even greater (a factor of 20).
- Uncertainty associated with the environmental impact can become smaller with the FBR HLW than with PWR HLW.

- The possibility of decreasing the environmental impact from the entire cycle, including legacy depleted uranium, by deployment of the FBR system has been indicated.
- ^{129}I could be one of the major contributor of the environmental impact because of its long half life and inert behavior in geologic environment.

I.4 Recommendations for Future Works

In the project in FY2005, fundamental models for environmental impact analysis have been established. The following tasks would strengthen and deepen the understanding obtained in this year's project.

- Importance of the waste-conditioning model has been recognized. It determines the source conditions for the repository impact analysis. In the present analysis, various assumptions were made, including
  - Concentrations of process chemicals, such as Na and P in the high-level liquid waste stream from a separation process,
  - Concentrations of corrosion products

  These can be determined by more detailed process analyses for separation processes. These assumptions affect the results significantly.
- Constraints for the waste –conditioning model need to be more detailed. Six constraints were considered in the present analysis. Requirements for waste conditioning, such as those from interim storage of vitrified HLW, should be taken into account. Some of the constraints have been developed based on empirical relations (for example, vitrified HLW density vs. HLW compositions). Validity of such formulae should be checked.
- Regarding waste conditioning, TRU waste generation should be treated in more detailed manner. TRU waste would have different behavior in a different repository. To make a fair comparison among various fuel cycle options, TRU waste effects should be treated separately.
- Uncertainty analysis should be made statistically, by applying probability distribution functions for each parameter. Uncertainties associated not only with transport parameters considered in this study but also with radionuclide inventory would have significant impact.

II. Introduction

Performance of a geologic repository has been evaluated by an annual dose due to radionuclides released from the repository. Previous analyses showed the effects of Partitioning-and-Transmutation (P/T) systems on the performance of geologic disposal by comparing the values of annual dose. The annual dose is based on the local concentration of a radionuclide in groundwater and the radionuclide pathways in the biosphere. Because the radionuclide concentration in the groundwater is not directly related with the mass of the radionuclide disposed of in a repository especially for low-solubility elements, effects of P/T on the repository performance measured by the annual dose have been considered insignificant. In the previous studies at UCB [1][2], it was observed that the total mass of a radionuclide in the repository can significantly affect the local concentration in groundwater if multiple-canister array configuration is taken into account.

In the present study, the environmental impact measure is defined as the radiotoxicity of a radionuclide that has been released from failed waste canisters and exists in the region exterior to the repository, which is considered the environment. In the recent study [2][3], it was shown that the environmental impact of a geologic repository defined this way can be a sensitive measure that shows difference for differing repository design, solidified high-level wastes (HLW) properties, and initial mass loadings of radionuclides in the solidified HLW. The initial mass loading of a radionuclide in the solidified waste is primarily determined by the fuel cycle scheme and the conditions for the solidification process. Thus, the present impact measure is expected to reflect sensitively differences in fuel cycle, solidification process, and repository design.

In the present paper, results of an analytical study are presented for the effects of initial mass loading of important contributors on environmental impacts of a geologic repository for the combination of a water-saturated repository, PUREX type reprocessing, and borosilicate-glass HLW solidification.

The study consists of two major parts.

The first is development of analytical formulae for the environmental impact of a geologic repository as a function of the canister layout in the repository (such as the canister array configuration and the dimensions of engineered barriers), the mass-transport parameters in the repository (such as the groundwater pore velocity, the retardation factors, the diffusion coefficients, and the solubilities), the canister-performance parameters (the canister failure time

and the waste-matrix dissolution time), and the initial mass loading of radionuclides in a waste canister. Formulae have been developed for solubility-limited release and for congruent release of radionuclides from a dissolving waste matrix.

The second is development of the waste conditioning model [4]. The waste conditioning model determines the compositions and the initial mass loading in each waste canister by taking into account the constraints imposed on the waste solidification, such as the Na content, the Mo content, and the heat load. This model connects the fuel-cycle mass-flow model with the repository-impact assessment model.

With these models and formulae, we have obtained the quantitative relationship between the repository capacity and the environmental impact of a geologic repository with HLW from light-water reactors (LWR) and fast-breeder reactors (FBR).

We have furthermore investigated the effects of shifting from the present LWR system to a FBR system on the environmental impact from the fuel cycle as well as the repository.

III. Environmental Impact

III.1 Environmental Impact Measure

The environmental impact of a radionuclide included in the waste disposed of in a geologic repository is defined as the radio-toxicity index for the radionuclide mass existing in the environment. In this study, we consider the peak value.

The toxicity index is defined as the radioactivity of the radionuclide divided by the maximum permissible concentration (MPC) of the radionuclide for drinking [5]. The index represents the volume of water with which the radionuclide solution can be diluted to its MPC. The toxicity index considered here as the impact measure takes into account the mechanisms by which the radionuclides could be released from the repository. In this respect, the environmental impact defined here is remarkably different from the toxicity index of radionuclides in the waste.

By the aforementioned definition, the environmental impact I [m^3 of water] due to a certain radionuclide i contained in the waste canisters is written as[2]

$$I_i = \left(N_x N_y \hat{M}_i^o \right) P_i C_i , \tag{1}$$

where $N_x N_y$ is the total number of waste canisters placed in the repository (see Figure 1). $\hat{M}_i^o$ [kg-nuclide] is the initial mass loading of radionuclide i in one canister. Coefficient $\hat{C}_i$ expresses the toxicity of unit mass of the radionuclide, defined as

$$\hat{C}_i \left[\mathrm{m^3\text{-}water/kg\text{-}nuclide} \right] \equiv \frac{\hat{\lambda}_i \left[/\mathrm{s} \right] \cdot 1000 \left[\mathrm{g/kg} \right] \cdot N_A \left[/\mathrm{mol} \right]}{M_i \left[\mathrm{g/mol} \right] \cdot 3.7 \times 10^{10} \left[\mathrm{Bq/Ci} \right] \cdot \left(\mathrm{MPC} \right)_i \left[\mathrm{Ci/m^3} \right]} \tag{2}$$

where $\hat{\lambda}_i$, Mi, and (MPC)i are the decay constant, the molecular mass, and the MPC of nuclide i, respectively. N_A is the Avogadro's number. The factor P_i is the ratio between the total initial mass loading $\left(N_x N_y \hat{M}_i^o \right)$ of radionuclide i in the repository to the peak mass of the radionuclide existing in the environment.

---

[2] Note that the parameters with physical dimensions are denoted with ^ symbols, whereas the non-dimensionalized parameters are denoted without it.

III.2 Radionuclide Transport in Repository

Radionuclide-transport models were recently developed [1][2][6], where multiple waste-canisters and their spatial configuration were incorporated by considering an array of compartments each containing a waste matrix, a buffer, and a near-field rock (NFR) region (Figure 1). It is assumed that each canister has identical mass loadings of radionuclides.

The repository consists of as many compartments as the number of waste canisters placed in the repository. For more detail about mathematical formulations and assumptions, the reader is referred to [1][2][6]. Brief summaries of the model and the findings are given here for readers' convenience.

The waste matrix, together with radionuclides contained in the matrix, starts to dissolve by pore-water in the buffer. The concentration of an actinide species in the pore-water at the waste-matrix dissolution location is limited by its solubility. Soluble species including most of fission products are released congruently with the dissolution of the waste matrix. Radionuclides are assumed to be transported through the pore-water in the buffer region by molecular diffusion, and then released into the NFR region. The buffer and the NFR are assumed to be homogeneously porous.

An array of multiple compartments in the repository is considered to be immersed in the parallel water stream[3]. It is assumed that there is no net mass transport through the interface between two parallel adjacent arrays. Groundwater is assumed to flow through the NFR at a constant, uniform velocity. A radionuclide released from the buffer is transported by advection through the NFR. Hydrodynamic dispersion is treated by an array of multiple compartments in the present model [1][6]. Linear sorption isotherms between the solid phase and the pore-water phase in the buffer and in the NFR are also assumed.

Uncontaminated water enters the NFR of the first compartment in the array. The water in the pores of the NFR is contaminated by the radionuclide released from the waste matrix and its transport through the buffer by diffusion. Contaminated water in the NFR continues to flow into the NFR of the second compartment in the array, and contacts with the buffer there. This

---

[3] This is one of the major differences between a water-saturated repository and the Yucca Mountain Repository (YMR), which is placed in the region above the water table. In YMR, groundwater flows vertically. Because each waste package is isolated hydrologically, interference among adjacent fractures can be neglected [7].

water gets additionally contaminated by radionuclides released from the second canister. In this fashion, the groundwater flowing in the array through the NFR is assumed to be increasingly contaminated before it finally flows out of the repository from the NFR of the end compartment.

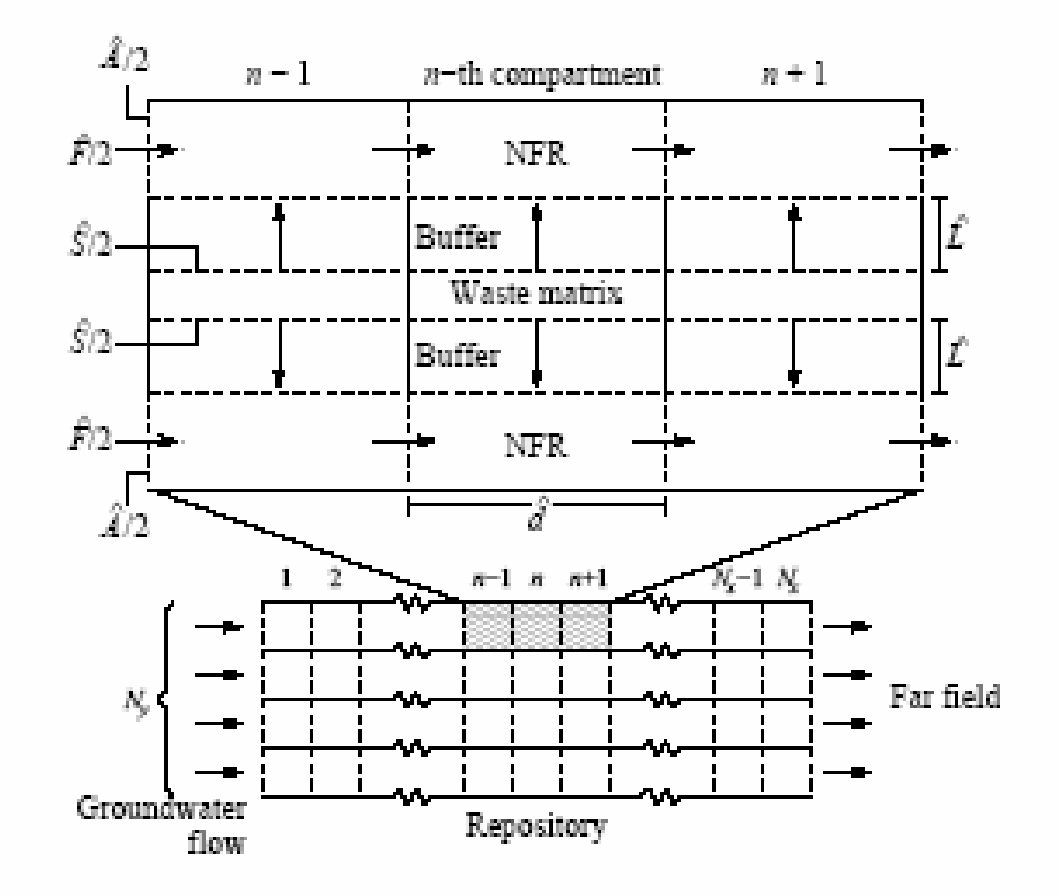

Figure 1: A two-dimensional array configuration of a geologic repository. There are N_y rows, each containing N_x waste canisters in the water-flow direction. The numbers N_x and N_y do not have to be the same as actual repository configuration. The number N_x should be determined by considering hydrological connection among canisters. Thus, a repository would consist of many rows with different N_x. The number N_y then should be determined to match the total number of canisters, i.e., total number of canisters = $\sum_{j=1}^{N_y} N_{x,j}$. In this study, however, all the rows consist of the same number N_x of hydrologically connected canisters.

III.3 Formulae for Peak mass Factor P

Formulations for the factor *P* have been developed separately for congruent-release radionuclides and for solubility-limited-release radionuclides. The factor *P* expresses the reduction of the mass of the radionuclide due to confinement by the repository. As the repository confinement capability improves, this factor decreases.

Utilizing the formulae for the release rates derived in [1] [2] and [6], mathematical expressions for the radionuclide mass in the environment have been obtained in this study by integrating the release rates with respect to time while taking into account the radioactive decay loss in the environment. Then, the factor *P* have been formulated by normalizing the peak value of the radionuclide mass in the environment released from the repository containing the total of $N_x N_y$ canisters by the total initial mass loading $\left(N_x N_y \hat{M}^o\right)$ in $N_x N_y$ canisters.

For the congruent release, the formulae have been obtained as shown in Table I based on the results of [6] for the following non-dimensionalized parameters:

$$T_L \equiv \hat{T}_L \Big/ \hat{T}_1 \,,\ \lambda \equiv \hat{\lambda}\hat{T}_1, \tag{3}$$

where
$$\hat{T}_1 \equiv \frac{\hat{\xi}}{\hat{F}},\ \ \hat{\xi} \equiv \hat{V}_R + \hat{V}_B,\ \hat{V}_R \equiv R\varepsilon_p \hat{V},\ \hat{V}_B \equiv K\varepsilon \hat{S}\hat{L}\,. \tag{4}$$

$\hat{T}_L$ is the dissolution time [yr] of the waste matrix, $\hat{F}$ the flow rate [m^3/yr] of groundwater through a row of N_x compartments, *R* and *K* the retardation factors of the radionuclide in the near field rock and in the buffer, respectively, ε_p and ε the porosities of the near-field rock and the buffer, respectively, $\hat{V}$ the volume [m^3] of the near field rock allocated for one compartment. For $\hat{S}$ and $\hat{L}$, see Figure 1.

Table I: Formulae for Peak Mass Factor P for Congruent Release

<table>
<tr><td colspan="2">$N_x < T_L$</td><td colspan="2">$T_L < N_x$</td></tr>
<tr><td>$1/\lambda < N_x/2$</td><td>$P = \dfrac{1}{2T_L N_x}\left(\dfrac{2}{\lambda}\right)^2 e^{-2}$</td><td>$1/\lambda < T_L/2$</td><td>$P = \dfrac{1}{2T_L N_x}\left(\dfrac{2}{\lambda}\right)^2 e^{-2}$</td></tr>
<tr><td>$N_x/2 < 1/\lambda < T_L - N_x/2$</td><td>$P = \dfrac{1}{\lambda T_L}\exp\left[-\left(1+\dfrac{\lambda N_x}{2}\right)\right.$</td><td>$T_L/2 < 1/\lambda < N_x - T_L/2$</td><td>$P = \dfrac{1}{\lambda N_x}\exp\left[-\left(1+\dfrac{\lambda T_L}{2}\right)\right.$</td></tr>
<tr><td>$T_L - N_x/2 < 1/\lambda$</td><td></td><td>$N_x - T_L/2 < 1/\lambda$</td><td></td></tr>
<tr><td colspan="4">$P = \dfrac{\sqrt{1+2T_L N_x \lambda^2}-1}{\lambda^2 T_L N_x}\exp\left[-\lambda\left(N_x+T_L\right)-1+\sqrt{1+2T_L N_x \lambda^2}\right]$</td></tr>
</table>

In the above formulation for congruent release nuclides, the quantity, $\hat{T}_1$, can be considered as the average residence time of a nuclide in a compartment. The quantity $\hat{\xi}$ represents the total capacity of a compartment for storing a nuclide, including sorption on to solid phases in the compartment.

For the solubility-limited release, the formulae have been obtained as shown in Table II based on the results of [2] for the following non-dimensionalized parameters:

$$\alpha \equiv \frac{\hat{T}_R \hat{D}}{K\hat{L}^2},\ \lambda' \equiv \hat{\lambda}\hat{T}_R,\ \sigma \equiv \frac{\hat{V}_B \hat{C}^*}{\hat{M}^o},\ \mu \equiv \hat{V}_B \Big/ \hat{V}_R, \tag{5}$$

and

$$\kappa \equiv \sqrt{\lambda' \Big/ \alpha},\ \beta \equiv \frac{\alpha\kappa}{\sinh\kappa},\ \zeta \equiv \lambda' + \beta\mu\cosh\kappa,\ \gamma \equiv \frac{1}{1+\zeta}. \tag{6}$$

Among these non-dimensionalized parameters, the first four shown in (5) are essential that determine the transport behavior of the nuclide in the repository region. Note that non-dimensionalization applied for the decay constant is different from that has been considered for congruent release case. Compare with eq. (3).

The quantity $\hat{T}_R \equiv \hat{V}_R \Big/ \hat{F}$, is considered as the nuclide residence time in the NFR of a compartment. $\hat{D}$ is the diffusion coefficient in the buffer, and $\hat{C}^*$ the solubility of the nuclide.

In Table II, the normalized time T is considered as the normalized depletion time of the nuclide from the waste form region in a compartment. This is determined by obtaining the normalized time when the normalized mass m_W of the nuclide in the canister becomes zero, and can be obtained by solving $m_W(T) = 0$ numerically, where

$$m_W(t) = \exp(-\lambda' t) + \frac{\beta\sigma}{\lambda'}\left[\frac{\mu\beta}{\zeta} - \cosh(\kappa)\right]\left[1 - \exp(-\lambda' t)\right] + \frac{\sigma\beta}{\zeta}\frac{\exp(-\zeta t) - \exp(-\lambda' t)}{\cosh(\kappa)}, \tag{7}$$

$$0 \le t \le T$$

Numerical solution of the above equation has been carried out by the Newton-Raphson method.

Computer codes for numerical evaluation of P factors (Table I and Table II) have been developed in FORTRAN.

Table II: Formulae for Peak Mass Factor P for Solubility-Limited Release

For $N_x < T$, $P = \left[A + a\left\{ \tau - \frac{\tau^2}{2N_x} \right\} \right] \exp\left(-\lambda' \tau\right)$

$$a = \frac{\sigma \bar{C}_{N_x}}{\mu N_x}, \quad b = N_x + \frac{1}{\lambda'}, \quad \tau = b - \sqrt{b^2 - \frac{2N_x}{\lambda'} + \frac{2N_x}{a} A},$$

$$\bar{C}_{N_x} = \frac{\mu\beta}{\zeta}\left(1 - \gamma^{N_x}\right), \quad T_{N_x} = N_x + \frac{1}{\lambda'} \ln\left[1 + \frac{\lambda' m_w\left(N_x\right)}{\bar{q}} \right],$$

$$A = \left\{ B - \frac{a}{\lambda'} \right\} \exp\left(-\lambda' \left(T_{N_x} - N_x \right) \right) + \frac{a}{\lambda'}, \quad \bar{q} = \beta\sigma\left(\cosh\kappa - \bar{C}_{N_x} \right)$$

$$B = \frac{\sigma\beta}{\zeta N_x}\left[\frac{1}{\lambda'} + \frac{\zeta}{\lambda'\left(\lambda' - \zeta\right)} \exp\left(-\lambda' N_x\right) - \frac{1}{\lambda' - \zeta} \exp\left(-\zeta N_x\right) \right]$$

For $N_x > T$, $P = \left[A + a\left\{ \tau - \frac{\tau^2}{2T} \right\} \right] \exp\left(-\lambda' \tau\right)$

$$a = \frac{\sigma C_{N_x}}{\mu N_x}, \quad b = T + \frac{1}{\lambda'}, \quad \tau = b - \sqrt{b^2 - \frac{2T}{\lambda'} + \frac{2T}{a} A},$$

$$C_{N_x} = \frac{\mu\beta}{\zeta}\left[1 - \exp\left(-\zeta T\right) \right] \exp\left(-\lambda' \left(N_x - T \right) \right),$$

$$A = B \exp\left(-\lambda' \left(N_x - T \right) \right) \left[B + \left(N_x - T \right) \frac{\sigma}{N_x} \frac{\beta}{\zeta} \left(1 - \exp\left(-\zeta T\right) \right) \right],$$

$$B = \frac{\sigma\beta}{\zeta N_x}\left[\frac{1}{\lambda'} + \frac{\zeta}{\lambda'\left(\lambda' - \zeta\right)} \exp\left(-\lambda' T\right) - \frac{1}{\lambda' - \zeta} \exp\left(-\zeta T\right) \right]$$

IV. Waste Conditioning Model

We have developed a mathematical model which determines the composition of a solidified HLW in a canister and the number of HLW canisters per unit mass of irradiated fuel, in such a way that the mass M_W of waste oxides included in one canister is maximized while satisfying several constraints. See Figure 2 and also [4].

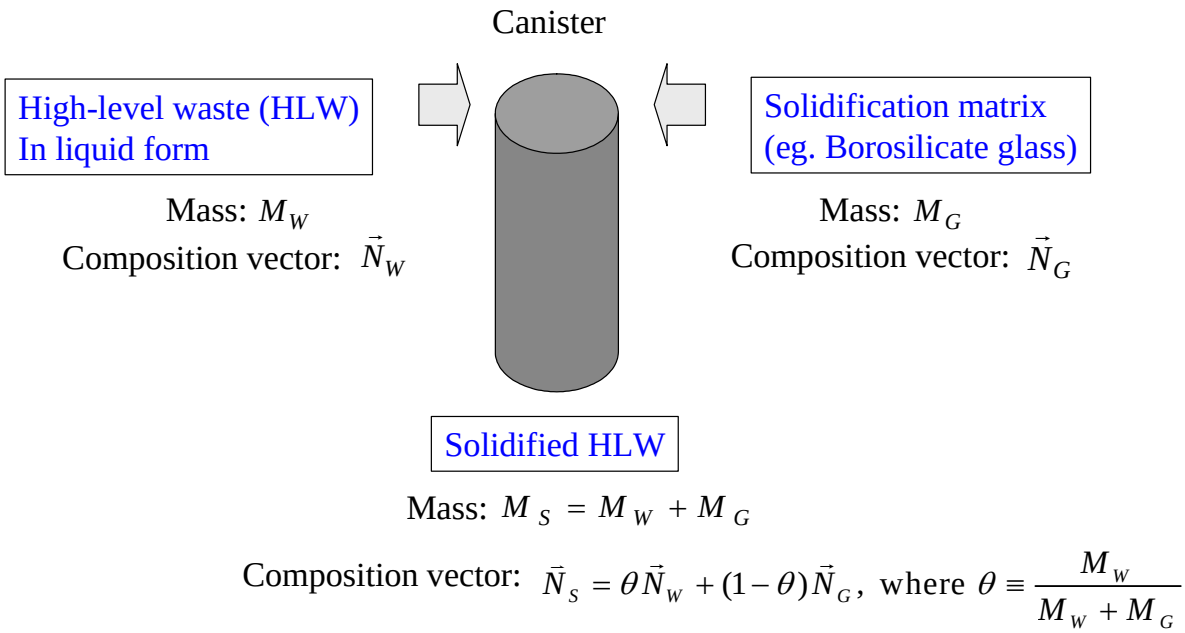

Figure 2: Conceptual diagram for optimization of waste loading in HLW solidification.

IV.1 Linear-Programming Problem

The mass of the solidified HLW in a single canister is the sum of M_W and the mass M_G of matrix material, such as borosilicate glass frit. If the composition vectors $\vec{N}_W$ for the waste oxides and $\vec{N}_G$ for the matrix material are known, the composition vector $\vec{N}_S$ of the solidified HLW is obtained as

$$\vec{N}_S = \frac{M_W}{M_W + M_G}\vec{N}_W + \frac{M_G}{M_W + M_G}\vec{N}_G . \qquad (8)$$

The number of HLW canisters for a unit mass of irradiated fuel can be calculated by dividing the mass of the HLW from processing a unit mass of irradiated fuel by M_W.

M_W and M_G can be determined by solving a linear programming problem. The objective

function, *f*, which is the mass M_W, is formulated as

$$\text{Maximize } f = M_W. \tag{9}$$

subject to a set of constraint inequalities expressed by

$$\mathbf{A}\begin{bmatrix} M_W \\ M_G \end{bmatrix} \le \mathbf{b}\,, \tag{10}$$

where **A** is the matrix of coefficients of constraint inequalities and **b** is the column vector of constants. If there are *n* constraints, matrix **A** is $n \times 2$ and vector **b** consists of *n* elements.

IV.2 Constraints

The objective function is subject to constraints for the borosilicate glass solidification. In this study, we have applied the model for the HLW vitrification process developed by JNC. Major constituents of high-level liquid wastes (HLLW) generating from PUREX reprocessing of PWR spent fuel are fission products, minor actinides, corrosion products, and process chemicals added in reprocessing. These are melted with glass frit for solidification.

For the canister for solidified HLW developed by JNC [8], we consider the following six constraints.

(1) The weight of the solidified HLW should not exceed 400 kg.
(2) The volume of the solidified HLW should not exceed the volume of an empty canister, 0.15 m^3.
(3) The total heat generation rate from the solidified HLW is limited by 2,300 W.
(4) the content of MoO_3 in waste matrix is limited by 2 wt% [11],
(5) the content of Na_2O in waste matrix is limited by 10 wt% [11], and
(6) the mass M_W should not exceed 30 wt% [12].

The first constraint is on the total mass of solidified HLW [8], written as

$$M_W + M_G \le 400 \ \ [\text{kg}]. \tag{11}$$

The second constraint is on the volume of the solidified HLW [8], yielding

$$\frac{M_W + M_G}{\rho_{WG}} \le 150 \ \ [\text{liter}], \tag{12}$$

where ρ_{WG} is the density of the solidified HLW. From Refs. [9] and [10], the density is formulated as

$$\rho_{WG} = 1230\left(\frac{M_W}{M_W + M_G}\right) + 2419 \quad [\mathrm{kg/m^3}]. \tag{13}$$

$$(M_W + M_G)^2 - (547.4M_W + 362.9M_G) \le 0 \tag{14}$$

By applying an empirical formula for ρ_{WG}, we have a quadratic inequality (14) for the constraint on the solidified waste volume limit. An LP model, however, requires constraints of a linear form and thus an approximate of (14) which is in a linear form needs to be employed. Figure 3 plots the quadratic inequality and its linear approximation. Dots represent the quadratic inequality and the solid line is its linear approximate. Hereafter, we utilize the following linearized constraint:

$$M_W + 1.508M_G \le 547.4 \ [\mathrm{kg}]. \tag{15}$$

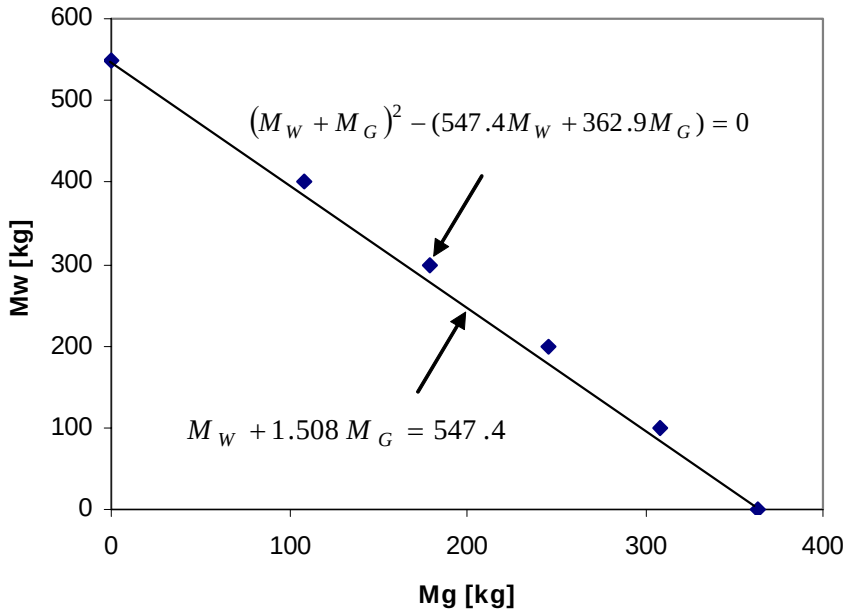

Figure 3: Linear approximation for the filled waste volume constraint

Constraint (3) is formulated by summing the decay heat of each isotope, which is expressed in terms of the composition vector $\vec{N}_W$ for the waste oxides, the decay heat and the decay constant of each nuclide. The third constraint is on the heat generation [8]:

$$\zeta M_W \le 2300 \quad [\mathrm{W}], \tag{16}$$

where ζ [W/kg] is heat generation per unit mass of waste oxides. This can be calculated by the

composition vector $\bar{N}_W$ for the waste oxides, the mean energy release from the decay and the decay constant of each nuclide.

Constraint (4) is on the mass fraction of Mo oxide in the solidified HLW. It must be smaller than 2 wt% [11]. Therefore,

$$x_{W,MoO_3} M_W \le 0.02\left(M_W + M_G\right), \tag{17}$$

where x_{W,MoO_3} is the mass fraction of MoO_3 in waste oxides.

Constraint (5) is that the mass fraction of Na_2O must be smaller than 10 wt% [11]. formulated as

$$x_{W,Na_2O} M_W + x_{G,Na_2O} M_G \le 0.1\left(M_W + M_G\right). \tag{18}$$

Note that Na_2O would be included in the waste oxides as well as in the matrix material.

Constraint (6) is on the waste loading limit in the borosilicate glass to avoid phase separation. The mass fraction of the waste oxides in the solidified waste must be smaller than 25% [12]. Therefore,

$$M_W \le 0.25\left(M_W + M_G\right),$$

or

$$M_W \le 0.333 M_G \tag{19}$$

The maximum value of M_W that satisfies the constraints formulated as (11), (12), (15), (16), (17), (18), (19) and two more intrinsic constraints,

$$M_W \ge 0,\ M_G \ge 0, \tag{20}$$

is determined by a linear programming approach.

V. Numerical Results and Discussions

V.1 Waste Conditioning for PWR Spent Fuel Reprocessing

We have applied the waste conditioning model for the waste oxide that would be generated from reprocessing of PWR fuel with the initial enrichment of 4.0%, the burn-up of 28 GWd-thermal/MTU, the cooling time of 180 days after discharge from the reactor, and the cooling time of 5 years between reprocessing and solidification.

The loss fractions of uranium and plutonium into waste oxides are 0.604% and 0.2966%, respectively [13]. Other actinide elements (Np, Am, and Cm) are assumed to be completely transferred to the waste oxide. All fission-product (FP) radionuclides except for noble gas elements are transferred to the waste oxide. No gaseous element, such as I and He is assumed to be included in the waste oxide.[4]

Data shown in [13] have been assumed for concentrations of corrosion products and process chemical in the HLLW. It is assumed in this study that 22.3 kg-Na and 0.393 kg-P as process chemicals, and 4.2 kg-Fe, 1.1 kg-Ni, and 1.09 kg-Cr as corrosion products are contained in the liquid HLW generated from the separation process of 1 MT of heavy metal.

The isotopic composition vector $\vec{N}_W$ of the waste oxide has been numerically calculated by ORIGEN code. The mass of oxides for each element has been calculated by assuming the chemical forms of oxide (see Table III).

With these, the heat generation ζ per unit mass of waste oxides has been calculated as 9.65 W/kg as shown in Table III. Assuming that the radionuclides are all in oxide forms, the mass of waste oxide from 1 MT of the irradiated fuel is calculated to be 78.1 kg (see the bottom of Table III).

For the waste matrix material, the glass frit PF798 developed by JNC is assumed [9]. See Table IV. This gives the vector $\vec{N}_G$.

[4] We consider impact of ^{129}I, however, because although it is not included in HLW it will eventually be released into the environment due to its long half-life. Same for FBR case.

Table III: HLW Composition Vector and Decay Heat Calculation for HLW from 1 Metric Ton of PWR Spent Fuel

(4.0% enriched, 28 GWD-thermal/MT, 5 year cooling before solidification, 99.396% and 99.703% recovery for U and Pu, Process Chemicals and Corrosion Products are included.)

Element	Mass no.	Mass of isotope in HLW [g]	Isotope Mass fraction in HLW, x_M	Oxide form	Mass of oxide in HLW [g]	Oxide Mass fraction in HLW, x_{MOn}	Half-life [sec]	decay constant [1/sec]	decay energy [MeV]	Zeta (i) [W/kg]
Fission Products										
Ge	76	3.680E-01	4.711E-06	GeO	4.45E-01	5.70E-06	0	0	0	0
As	75	1.060E-01	1.357E-06	As_2O_3	1.40E-01	1.79E-06	0	0	0	0
Se	77	9.030E-01	1.156E-05	SeO_2	1.28E+00	1.64E-05	0	0	0	0
	78	2.040E+00	2.612E-05		2.88E+00	3.68E-05	0	0	0	0
	79	5.054E+00	6.470E-05		7.10E+00	9.09E-05	2.05E+12	3.38E-13	4.20E-02	1.120E-06
	80	1.166E+01	1.493E-04		1.63E+01	2.09E-04	0	0	0	0
	82	3.004E+01	3.846E-04		4.18E+01	5.35E-04	0	0	0	0
Rb	85	9.533E+01	1.220E-03	Rb_2O	1.04E+02	1.34E-03	0	0	0	0
	87	2.247E+02	2.876E-03		2.45E+02	3.14E-03	1.48E+18	4.68E-19	1.41E-01	2.100E-10
Sr	86	2.611E-01	3.343E-06	SrO	3.10E-01	3.97E-06	0	0	0	0
	88	3.326E+02	4.258E-03		3.93E+02	5.03E-03	0	0	0	0
	90	4.501E+02	5.762E-03		5.30E+02	6.79E-03	9.19E+08	7.55E-10	1.96E-01	9.117E-01
Y	89	4.369E+02	5.592E-03	Y_2O_3	5.55E+02	7.10E-03	0	0	0	0
	90	1.132E-01	1.449E-06		1.43E-01	1.84E-06	2.30E+05	3.01E-06	0.935	4.363E+00
Zr	90	7.879E+01	1.009E-03	ZrO_2	1.07E+02	1.37E-03	0	0	0	0
	91	5.592E+02	7.159E-03		7.56E+02	9.68E-03	0	0	0	0
	92	5.970E+02	7.642E-03		8.05E+02	1.03E-02	0	0	0	0
	93	6.626E+02	8.482E-03		8.91E+02	1.14E-02	4.83E+13	1.44E-14	1.96E-02	2.479E-06
	94	6.704E+02	8.582E-03		8.99E+02	1.15E-02	0	0	0	0
	96	7.121E+02	9.116E-03		9.49E+02	1.22E-02	0	0	0	0
Mo	95	6.968E+02	8.920E-03	MoO_3	1.05E+03	1.34E-02	0	0	0	0
	96	2.030E+01	2.598E-04		3.05E+01	3.90E-04	0	0	0	0
	97	7.018E+02	8.984E-03		1.05E+03	1.34E-02	0	0	0	0
	98	7.233E+02	9.260E-03		1.08E+03	1.38E-02	0	0	0	0
	100	8.080E+02	1.034E-02		1.20E+03	1.53E-02	0	0	0	0
Tc	99	7.300E+02	9.345E-03	Tc_2O_7	1.14E+03	1.46E-02	6.77E+12	1.04E-13	8.46E-02	8.000E-05
Ru	100	5.816E+01	7.445E-04	RuO_2	7.68E+01	9.83E-04	0	0	0	0
	101	6.532E+02	8.362E-03		8.60E+02	1.10E-02	0	0	0	0
	102	6.212E+02	7.953E-03		8.16E+02	1.04E-02	0	0	0	0
	104	3.948E+02	5.054E-03		5.16E+02	6.61E-03	0	0	0	0
	106	2.638E+00	3.377E-05		3.43E+00	4.40E-05	3.18E+07	2.18E-08	0.01003	6.706E-03
Rh	103	3.960E+02	5.069E-03	Rh_2O_3	4.88E+02	6.25E-03	0	0	0	0
Pd	104	1.367E+02	1.749E-03	PdO	1.58E+02	2.02E-03	0	0	0	0
	105	2.845E+02	3.641E-03		3.28E+02	4.20E-03	0	0	0	0
	106	2.369E+02	3.033E-03		2.73E+02	3.49E-03	0	0	0	0
	107	1.430E+02	1.830E-03		1.64E+02	2.10E-03	2.05E+14	3.38E-15	1.00E-02	5.569E-08
	108	9.624E+01	1.232E-03		1.10E+02	1.41E-03	0	0	0	0
	110	3.174E+01	4.064E-04		3.64E+01	4.66E-04	0	0	0	0
Ag	109	4.180E+01	5.351E-04	Ag_2O	4.49E+01	5.75E-04	0	0	0	0
Cd	110	1.095E+01	1.402E-04	CdO	1.25E+01	1.61E-04	0	0	0	0
	111	1.300E+01	1.664E-04		1.49E+01	1.90E-04	0	0	0	0
	112	8.066E+00	1.033E-04		9.22E+00	1.18E-04	0	0	0	0
	113	1.103E-01	1.412E-06		1.26E-01	1.61E-06	0	0	0	0
	113m	9.776E-02	1.251E-06		1.12E-01	1.43E-06	0	0	0	0
	114	1.154E+01	1.478E-04		1.32E+01	1.69E-04	0	0	0	0
	116	4.527E+00	5.795E-05		5.15E+00	6.60E-05	0	0	0	0
In	115	1.110E+00	1.421E-05	In_2O_3	1.34E+00	1.72E-05	1.58E+22	4.39E-23	0.242	1.266E-16

Sn	115	1.231E-01	1.576E-06	SnO_2	1.57E-01	2.01E-06	0	0	0	0
	116	2.445E+00	3.131E-05		3.12E+00	3.99E-05	0	0	0	0
	117	3.263E+00	4.177E-05		4.16E+00	5.32E-05	0	0	0	0
	118	3.325E+00	4.257E-05		4.23E+00	5.41E-05	0	0	0	0
	119	3.296E+00	4.219E-05		4.18E+00	5.36E-05	0	0	0	0
	120	3.374E+00	4.319E-05		4.27E+00	5.47E-05	0	0	0	0
	122	3.730E+00	4.775E-05		4.71E+00	6.03E-05	0	0	0	0
	124	5.130E+00	6.567E-05		6.45E+00	8.26E-05	0	0	0	0
	126	1.111E+01	1.423E-04		1.39E+01	1.78E-04	3.15E+12	2.20E-13	1.14E+00	2.716E-05
Sb	121	3.115E+00	3.987E-05	Sb_2O_3	3.73E+00	4.78E-05	0	0	0	0
	123	3.838E+00	4.913E-05		4.59E+00	5.87E-05	0	0	0	0
	125	1.378E+00	1.764E-05		1.64E+00	2.10E-05	8.74E+07	7.93E-09	0.5274	5.683E-02
Te	122	2.781E-01	3.560E-06	TeO_2	3.51E-01	4.49E-06	0	0	0	0
	124	2.060E-01	2.637E-06		2.59E-01	3.32E-06	0	0	0	0
	125	1.060E+01	1.357E-04		1.33E+01	1.70E-04	0	0	0	0
	125m	3.703E-01	4.741E-06		4.65E-01	5.96E-06	5.01E+06	1.38E-07	1.42E-01	7.164E-02
	126	4.938E-01	6.321E-06		6.19E-01	7.93E-06	0	0	0	0
	128	8.333E+01	1.067E-03		1.04E+02	1.33E-03	0	0	0	0
	130	2.761E+02	3.534E-03		3.44E+02	4.41E-03	0	0	0	0
I	129	1.420E+02	1.818E-05							
Cs	133	1.002E+03	1.282E-02	Cs_2O	1.06E+03	1.36E-02	0	0	0	0
	134	1.247E+01	1.596E-04		1.32E+01	1.69E-04	6.51E+07	1.07E-08	1.717	2.098E+00
	135	2.972E+02	3.805E-03		3.15E+02	4.03E-03	7.26E+13	9.55E-15	5.63E-02	1.460E-06
	137	8.986E+02	1.150E-02		9.51E+02	1.22E-02	9.47E+08	7.30E-10	1.87E-01	1.102E+00
Ba	134	9.228E+01	1.181E-03	BaO	1.03E+02	1.32E-03	0	0	0	0
	135	1.243E+01	1.591E-04		1.39E+01	1.78E-04	0	0	0	0
	137	1.571E+02	2.011E-03		1.75E+02	2.25E-03	0	0	0	0
	138	1.178E+03	1.508E-02		1.31E+03	1.68E-02	0	0	0	0
La	139	1.080E+03	1.383E-02	La_2O_3	1.27E+03	1.62E-02	0	0	0	0
Ce	140	1.100E+03	1.409E-02	CeO_2	1.35E+03	1.73E-02	0	0	0	0
	142	1.007E+03	1.289E-02		1.23E+03	1.58E-02	3.31E+18	2.09E-19	0	0
	144	2.893E+00	3.703E-05		3.54E+00	4.53E-05	2.46E+07	2.82E-08	0.1119	7.822E-02
Pr	141	9.970E+02	1.276E-02	Pr_6O_{11}	1.20E+03	1.54E-02	0	0	0	0
Nd	142	1.569E+01	2.009E-04	Nd_2O_3	1.83E+01	2.35E-04	0	0	0	0
	143	7.722E+02	9.885E-03		9.02E+02	1.15E-02	0	0	0	0
	144	1.109E+03	1.420E-02		1.29E+03	1.66E-02	6.62E+22	1.05E-23	0	0
	145	6.191E+02	7.925E-03		7.22E+02	9.24E-03	0	0	0	0
	146	5.817E+02	7.446E-03		6.77E+02	8.67E-03	0	0	0	0
	148	3.186E+02	4.079E-03		3.70E+02	4.74E-03	0	0	0	0
	150	1.437E+02	1.839E-03		1.67E+02	2.13E-03	0	0	0	0
Pm	147	3.130E+01	4.007E-04	Pm_2O_3	3.64E+01	4.66E-04	8.28E+07	8.39E-09	6.05E-02	1.333E-01
Sm	147	1.843E+02	2.359E-03	Sm_2O_3	2.14E+02	2.75E-03	3.38E+18	2.05E-19	2.31	7.327E-10
	148	1.279E+02	1.637E-03		1.49E+02	1.90E-03	2.53E+23	2.74E-24	2.014	5.889E-15
	149	3.870E+00	4.954E-05		4.49E+00	5.75E-05	3.15E+23	2.20E-24	0	0
	150	2.660E+02	3.405E-03		3.09E+02	3.95E-03	0	0	0	0
	151	1.294E+01	1.657E-04		1.50E+01	1.92E-04	2.84E+09	2.44E-10	1.98E-02	5.101E-04
	152	1.179E+02	1.509E-03		1.37E+02	1.75E-03	0	0	0	0
	154	2.724E+01	3.487E-04		3.15E+01	4.03E-04	0	0	0	0
Eu	151	6.236E-01	7.983E-06	Eu_2O_3	7.23E-01	9.25E-06	0	0	0	0
	153	9.042E+01	1.158E-03		1.05E+02	1.34E-03	0	0	0	0
	154	1.735E+01	2.220E-04		2.01E+01	2.57E-04	2.71E+08	2.56E-09	1.51E+00	5.365E-01
	155	4.605E+00	5.895E-05		5.32E+00	6.81E-05	1.57E+08	4.43E-09	0.1227	1.990E-02
Gd	154	1.059E+01	1.355E-04	Gd_2O_3	1.22E+01	1.57E-04	0	0	0	0
	155	5.138E+00	6.578E-05		5.93E+00	7.60E-05	0	0	0	0
	156	3.442E+01	4.406E-04		3.97E+01	5.09E-04	0	0	0	0
	158	1.125E+01	1.440E-04		1.30E+01	1.66E-04	0	0	0	0
	160	8.098E-01	1.037E-05		9.31E-01	1.19E-05	0	0	0	0

Tb	159	1.190E+00	1.523E-05	Tb_2O_3	1.37E+00	1.75E-05	0	0	0	0
Dy	160	1.192E-01	1.526E-06	Dy_2O_3	1.37E-01	1.76E-06	0	0	0	0
	161	2.488E-01	3.186E-06		2.86E-01	3.66E-06	0	0	0	0
	162	2.084E-01	2.668E-06		2.39E-01	3.06E-06	0	0	0	0
	163	1.426E-01	1.825E-06		1.64E-01	2.09E-06	0	0	0	0
Actinides										
U	235	9.032E+01	1.156E-03	U_3O_8	1.07E+02	1.37E-03	2.22E+16	3.12E-17	4.42E+00	6.533E-08
	236	2.572E+01	3.292E-04		3.04E+01	3.89E-04	7.39E+14	9.38E-16	4.57E+00	5.760E-07
	238	5.694E+03	7.289E-02		6.71E+03	8.60E-02	1.41E+17	4.92E-18	4.28E+00	6.211E-07
Np	237	3.780E+02	4.839E-03	NpO_2	4.29E+02	5.49E-03	6.75E+13	1.03E-14	5.16E+00	1.044E-04
Pu	238	1.436E+00	1.839E-05	PuO_2	1.63E+00	2.09E-05	2.77E+09	2.50E-10	5.59E+00	1.040E-02
	239	1.531E+01	1.960E-04		1.74E+01	2.22E-04	7.59E+11	9.11E-13	5.20E+00	3.742E-04
	240	6.285E+00	8.045E-05		7.12E+00	9.12E-05	2.06E+11	3.35E-12	5.25E+00	5.682E-04
	241	1.933E+00	2.475E-05		2.19E+00	2.80E-05	4.54E+08	1.53E-09	5.23E-03	7.915E-05
	242	5.335E-01	6.829E-06		6.04E-01	7.73E-06	1.22E+13	5.68E-14	6.66E-02	2.627E-05
Am	241	3.885E+01	4.974E-04	Am_2O_3	4.27E+01	5.47E-04	1.36E+10	5.08E-11	5.60E+00	5.659E-02
	242 m	3.338E-01	4.273E-06		3.67E-01	4.70E-06	4.80E+09	1.45E-10	6.66E-02	1.644E-05
	243	2.171E+01	2.780E-04		2.39E+01	3.05E-04	2.33E+11	2.98E-12	5.42E+00	1.781E-03
Cm	242	3.234E-03	4.140E-08	Cm_2O_3	3.55E-03	4.55E-08	1.41E+07	4.92E-08	6.22E+00	5.043E-03
	243	1.396E-01	1.787E-06		1.53E-01	1.96E-06	8.99E+08	7.71E-10	6.19E+00	3.380E-03
	244	5.437E+00	6.960E-05		5.97E+00	7.65E-05	5.72E+08	1.21E-09	5.90E+00	1.962E-01
	245	1.770E-01	2.266E-06		1.94E-01	2.49E-06	2.68E+11	2.59E-12	5.60E+00	1.292E-05
	246	1.304E-02	1.670E-07		1.43E-02	1.83E-07	1.49E+11	4.65E-12	5.52E+00	1.679E-06
Total (FP+Ac)		*3.074E+04*	*3.935E-01*		*3.79E+04*	*4.86E-01*				**9.652E+0**
Process Chemicals										
Na		2.230E+04	2.855E-01	Na_2O	3.01E+04	3.85E-01				
P		3.930E+02	5.032E-03	P_2O_5	1.10E+03	1.41E-02				
Corrosion Products										
Fe		4.200E+03	5.378E-02	Fe_2O_3	6.00E+03	7.69E-02				
Ni		1.100E+03	1.408E-02	NiO	1.40E+03	1.79E-02				
Cr		1.090E+03	1.396E-02	Cr_2O_3	1.59E+03	2.04E-02				
Oxygen to form oxides										
Oxygen		1.828E+04	2.340E-01							
Grand Total		7.810E+04	1		**7.81E+04**	**1**				

Table IV: Composition of the Glass Frit, PF798, Developed by JNC [9]

Oxide	wt%
SiO_2	62.30
B_2O_3	19.00
Al_2O_3	6.70
Li_2O	4.00
CaO	4.00
ZnO	4.00

The constraints are summarized as follow:

$$M_W + M_G \le 400. \tag{11}$$

$$M_W + 1.508 M_G \le 547.4. \tag{15}$$

With ζ = 9.65 [W/kg],

$$M_W \le 238.3. \tag{21}$$

The mass fraction x_{W,MoO_3} of MoO_3 is obtained from Table III as 1.34E-02 + 3.90E-04 + 1.34E-02 + 1.38E-02 + 1.53E-02 = 5.63E-02. Therefore,

$$M_W \le 0.551 M_G , \tag{22}$$

The mass fraction of Na_2O in HLW is obtained from Table III as 3.85E-01. The mass fraction in glass frit is zero. Therefore,

$$M_W \le 0.351 M_G . \tag{23}$$

Also from constraint (6), $$M_W \le 0.333 M_G \tag{19}$$

Figure 4 shows graphically how the maximum waste loading has been determined. The maximum HLW loading M_W is observed at the intersection between the lines given by (15) and (19), obtained as (M_W ,MG) = (99.0 kg, 297 kg).

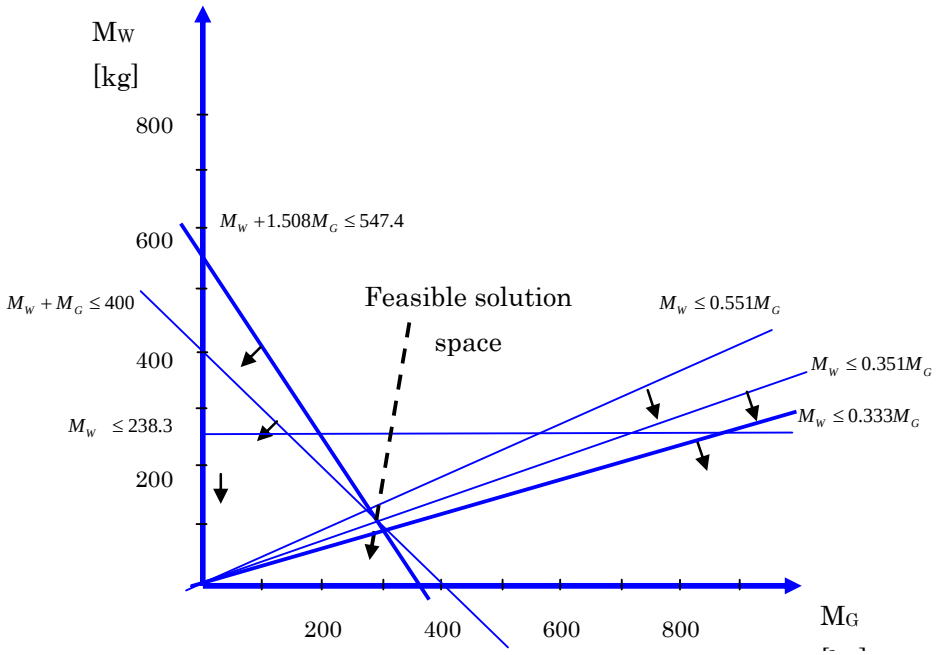

Figure 4: Graphical solution for optimum PWR-HLW conditioning

With these values, the HLW composition vector (8) is written as

$$\vec{N}_S = 0.25\vec{N}_W + 0.75\vec{N}_G . \tag{24}$$

With the optimum waste loading M_w = 99.0 kg, the number of waste canisters per MT of spent fuel is calculated to be 78.1/99.0 = 0.79 canister/MT. With the assumed burn-up of 28 GW·day-thermal/MTU and the heat-to-electricity conversion efficiency of 33%, the electricity per canister is calculated to be 28/0.79 x 0.33 = 11.7 GW·day-electric/canister. If a repository

designed for 40,000 canisters is filled with canisters of the loading obtained here, assuming that the reactors were operated with the capacity factor of 90%, the repository capacity is equivalent to 1420 GW·yr[5] of electricity generation.

V.2 Waste Conditioning for FBR Spent Fuel Reprocessing

We have also applied the waste conditioning model for the waste oxide that would be generated from reprocessing of FBR fuel. The thermal and electric output of the reactor assumed here are 3570 MW-thermal and 1500 MW-electric, respectively. For these power outputs for 510 days operation period, 1.07E+04 kg (core fuel), 9.33E+03 kg (axial blanket fuel), 9.03E+03 kg (radial blanket fuel), or total 2.91E+04 kg of heavy metal are assumed. Therefore, electricity generation of 1500 x 510 = 765 GW·day -electric is assumed to be made by 29.1 MTHM of fuel, or 26.3 GW·day-electric/MTHM. For thermal output, similarly, 62.6 GW·day-thermal/MTHM is obtained. With the input data files shown in Appendix, we have calculated the compositions of the spent fuels (core, axial and radial) at the time of discharge from the reactor. The results are shown in Table V.

The loss fraction of all actinides (U, Pu, Np, Am, and Cm) into waste oxides is assumed to be 0.1%. All fission-product (FP) radionuclides except for noble gas (Kr and Xe) elements are transferred to the waste oxide. No gaseous element, such as I and He, is assumed to be included in the waste oxide.

Data shown in [13] have been used for concentrations of corrosion products and process chemical in the HLLW. It is assumed in this study that 22.3 kg-Na and 0.393 kg-P as process chemicals, and 4.2 kg-Fe, 1.1 kg-Ni, and 1.09 kg-Cr as corrosion products are contained in the liquid HLW generated from the separation process of 1 MT of heavy metal. The masses of these elements are added to the HLW, proportional to the mass of heavy metal to be reprocessed.[6]

Once the mass of process chemicals, corrosion products and radionuclides have been determined, the mass of oxides for each element has been calculated by assuming the chemical

---

[5] In the H12 study for repository performance assessment by JNC [8], 1.25 canisters/MTU is assumed for the burn-up of 45,000 MWday/MTU. Assuming the same heat-to-electricity conversion efficiency and the capacity factor, the repository with 40,000 canisters is equivalent to 1440 GW-year. This comparison shows that increasing the burn-up of the fuel does not save the repository capacity.

[6] The reprocessing would be separately made for core and blanket fuels, because of largely different burn-ups. But, in this evaluation, all three types of fuels are mixed and reprocessed together.

forms of oxide (see Table V). The total mass of HLW in oxide forms is obtained as 3150 kg for 29.1 MTHM reprocessed, resulting in 108 kg of HLW oxides/MTHM. The heat generation ζ per unit mass of waste oxides has been calculated as 11.4 W/kg, as shown in Table V.

The constraints are summarized as follow:

$$M_W + M_G \le 400. \tag{11}$$

$$M_W + 1.508 M_G \le 547.4. \tag{15}$$

With ζ = 11.4 [W/kg],

$$M_W \le 201.8. \tag{25}$$

The mass fraction x_{W,MoO_3} of MoO_3 is obtained from Table V as 1.57E-02 + 1.11E-03 + 1.61E-02 + 1.90E-02 + 2.10E-02 = 7.92E-02. Therefore,

$$M_W \le 0.338 M_G, \tag{26}$$

The mass fraction of Na_2O in HLW is obtained from Table V as 2.78E-01. The mass fraction in glass frit is zero. Therefore,

$$M_W \le 0.562 M_G. \tag{27}$$

And

$$M_W \le 0.333 M_G. \tag{19}$$

Figure 5 shows graphically how the maximum waste loading has been determined. The maximum HLW loading M_W is observed at the intersection between the lines given by (15) and (19), obtained as (M_W ,MG) = (99.0 kg, 297 kg). It is observed that the Mo constraint has become closer to the waste loading constraint.

With the optimum waste loading M_w = 99.0 kg, the number of waste canisters per MTHM is calculated to be 108/99.0 = 1.09 canister/MTHM. With the assumed electricity output of 26.3 GW·day-e/MTHM, the electricity per canister is calculated to be 26.3/1.09 = 24.1 GW·day-e/canister. If a repository designed for 40,000 canisters is filled with canisters of the loading obtained here, assuming that the reactors were operated with the capacity factor of 90%, the repository capacity is equivalent to 2940 GW·yr of electricity generation, twice as large as that for the PWR case.

Table V: HLW Composition Vector and Decay Heat Calculation for 1500 MWe FBR Operation

(4 year cooling before solidification, 99.9% recovery of actinide for recycle, 100% recovery of FPs, Process Chemicals and Corrosion Products are included.)

Element	Mass no.	Mass of isotope in spent fuel [g]				Mass of isotope in HLW in oxide forms [g]	Isotope Mass fraction in HLW, x_M	Oxide form	Mass of oxide in HLW	Oxide Mass fraction in HLW, x_{MOn}	Half-life [sec]	decay constant [1/sec]	decay energy [MeV]	Zeta (i) [W/kg]
		Core	Axial Blanket	Radial Blanket	Sum									
Ge	74	9.76E+00	3.29E-01	6.44E-02	1.01E+01	1.01E+01	3.22E-06	GeO	1.23E+01	3.92E-06	-	0		0
	76	3.19E+01	1.04E+00	2.13E-01	3.32E+01	3.32E+01	1.05E-05		4.01E+01	1.28E-05	-	0		0
As	75	1.49E+01	5.57E-01	1.12E-01	1.55E+01	1.55E+01	4.93E-06	As2O3	2.05E+01	6.51E-06	-	0		0
Se	76	1.42E+00	1.37E-02	7.75E-04	1.43E+00	1.43E+00	4.54E-07	SeO2	2.03E+00	6.45E-07	-	0		0
	77	5.87E+01	1.90E+00	3.94E-01	6.10E+01	6.10E+01	1.94E-05		8.64E+01	2.74E-05	-	0		0
	78	1.22E+02	3.41E+00	7.10E-01	1.26E+02	1.26E+02	3.99E-05		1.77E+02	5.63E-05	-	0		0
	79	2.51E+02	7.78E+00	1.53E+00	2.60E+02	2.60E+02	8.26E-05		3.65E+02	1.16E-04	2.05E+12	3.38E-13	4.20E-02	1.43E-06
	80	3.97E+02	1.22E+01	2.55E+00	4.11E+02	4.11E+02	1.31E-04		5.76E+02	1.83E-04	-	0		0
	82	9.77E+02	3.41E+01	6.95E+00	1.02E+03	1.02E+03	3.23E-04		1.42E+03	4.50E-04	-	0		0
Rb	85	3.04E+03	9.56E+01	1.99E+01	3.16E+03	3.16E+03	1.00E-03	Rb2O	3.45E+03	1.10E-03	-	0		0
	87	6.82E+03	2.13E+02	4.48E+01	7.07E+03	7.07E+03	2.25E-03		7.72E+03	2.45E-03	1.48E+18	4.68E-19	1.41E-01	1.64E-10
Sr	86	1.62E+02	1.03E+00	7.05E-02	1.63E+02	1.63E+02	5.17E-05	SrO	1.93E+02	6.13E-05	-	0		0
	88	8.93E+03	2.96E+02	6.33E+01	9.29E+03	9.29E+03	2.95E-03		1.10E+04	3.49E-03	-	0		0
	90	1.17E+04	3.75E+02	8.03E+01	1.21E+04	1.21E+04	3.85E-03		1.43E+04	4.53E-03	9.19E+08	7.55E-10	1.96E-01	0.609
Y	89	1.17E+04	3.85E+02	8.17E+01	1.21E+04	1.21E+04	3.85E-03	Y2O3	1.54E+04	4.89E-03	-	0		0
	90	2.92E+00	9.39E-02	2.02E-02	3.04E+00	3.04E+00	9.65E-07		3.85E+00	1.22E-06	2.30E+05	3.01E-06	0.935	2.907
Zr	90	2.11E+03	6.87E+01	1.48E+01	2.19E+03	2.19E+03	6.96E-04	ZrO2	2.97E+03	9.44E-04	-	0		0
	91	1.60E+04	5.11E+02	1.07E+02	1.66E+04	1.66E+04	5.27E-03		2.24E+04	7.13E-03	-	0		0
	92	1.98E+04	5.86E+02	1.20E+02	2.05E+04	2.05E+04	6.52E-03		2.77E+04	8.79E-03	-	0		0
	93	2.45E+04	6.99E+02	1.40E+02	2.53E+04	2.53E+04	8.05E-03		3.41E+04	1.08E-02	4.83E+13	1.44E-14	1.96E-02	2.35E-06
	94	2.73E+04	6.99E+02	1.37E+02	2.81E+04	2.81E+04	8.93E-03		3.77E+04	1.20E-02	-	0		0
	96	3.25E+04	8.37E+02	1.61E+02	3.35E+04	3.35E+04	1.06E-02		4.46E+04	1.42E-02	-	0		0
Mo	95	3.18E+04	8.91E+02	1.74E+02	3.29E+04	3.29E+04	1.04E-02	MoO3	4.95E+04	1.57E-02	-	0		0
	96	2.31E+03	1.43E+01	8.77E-01	2.32E+03	2.32E+03	7.38E-04		3.49E+03	1.11E-03	-	0		0
	97	3.28E+04	8.65E+02	1.65E+02	3.38E+04	3.38E+04	1.07E-02		5.06E+04	1.61E-02	-	0		0
	98	3.90E+04	9.32E+02	1.74E+02	4.01E+04	4.01E+04	1.28E-02		5.98E+04	1.90E-02	-	0		0
	100	4.35E+04	1.04E+03	1.94E+02	4.47E+04	4.47E+04	1.42E-02		6.62E+04	2.10E-02	-	0		0
Tc	99	3.66E+04	9.54E+02	1.80E+02	3.78E+04	3.78E+04	1.20E-02	Tc2O7	5.91E+04	1.88E-02	6.77E+12	1.04E-13	8.46E-02	0.000102
Ru	100	4.42E+03	2.39E+01	1.33E+00	4.44E+03	4.44E+03	1.41E-03	RuO2	5.87E+03	1.86E-03	-	0		0
	101	4.01E+04	1.03E+03	1.91E+02	4.13E+04	4.13E+04	1.31E-02		5.44E+04	1.73E-02	-	0		0

	102	4.90E+04	1.08E+03	1.91E+02	5.03E+04	5.03E+04	1.60E-02		6.60E+04	2.10E-02	-	0		0
	104	4.39E+04	9.35E+02	1.58E+02	4.50E+04	4.50E+04	1.43E-02		5.89E+04	1.87E-02	-	0		0
	106	5.17E+02	1.00E+01	1.64E+00	5.29E+02	5.29E+02	1.68E-04		6.89E+02	2.19E-04	3.18E+07	2.18E-08	0.01003	0.03338
Rh	103	4.05E+04	1.00E+03	1.75E+02	4.17E+04	4.17E+04	1.33E-02	Rh2O3	5.14E+04	1.63E-02	-	0		0
Pd	104	8.10E+03	3.50E+01	1.94E+00	8.14E+03	8.14E+03	2.59E-03	PdO	9.39E+03	2.98E-03	-	0		0
	105	3.11E+04	7.13E+02	1.19E+02	3.20E+04	3.20E+04	1.02E-02		3.68E+04	1.17E-02	-	0		0
	106	3.73E+04	5.99E+02	9.21E+01	3.80E+04	3.80E+04	1.21E-02		4.37E+04	1.39E-02	-	0		0
	107	2.11E+04	3.79E+02	5.98E+01	2.15E+04	2.15E+04	6.84E-03		2.47E+04	7.86E-03	2.05E+14	3.38E-15	1.00E-02	2.080E-07
	108	1.89E+04	2.76E+02	4.20E+01	1.92E+04	1.92E+04	6.10E-03		2.20E+04	7.00E-03	-	0		0
	110	5.20E+03	1.04E+02	1.71E+01	5.32E+03	5.32E+03	1.69E-03		6.10E+03	1.94E-03	-	0		0
Ag	109	1.12E+04	1.99E+02	3.10E+01	1.14E+04	1.14E+04	3.64E-03	Ag2O	1.23E+04	3.90E-03	-	0		0
Cd	110	1.65E+03	5.91E+00	2.86E-01	1.66E+03	1.66E+03	5.27E-04	CdO	1.90E+03	6.03E-04	-	0		0
	111	3.13E+03	7.30E+01	1.26E+01	3.22E+03	3.22E+03	1.02E-03		3.68E+03	1.17E-03	-	0		0
	112	2.13E+03	5.62E+01	9.92E+00	2.20E+03	2.20E+03	6.99E-04		2.51E+03	7.99E-04	-	0		0
	113	1.38E+03	4.64E+01	8.56E+00	1.44E+03	1.44E+03	4.56E-04		1.64E+03	5.21E-04	-	0		0
	113	2.51E+01	5.86E-01	1.05E-01	2.58E+01	2.58E+01	8.19E-06		2.94E+01	9.34E-06	-	0		0
	114	1.10E+03	3.84E+01	7.07E+00	1.15E+03	1.15E+03	3.65E-04		1.31E+03	4.16E-04	-	0		0
	116	7.65E+02	3.38E+01	6.44E+00	8.05E+02	8.05E+02	2.56E-04		9.16E+02	2.91E-04	-	0		0
In	115	4.27E+02	3.53E+01	7.31E+00	4.70E+02	4.70E+02	1.49E-04	In2O3	5.68E+02	1.80E-04	1.58E+22	4.39E-23	0.242	1.328E-15
Sn	115	3.69E+01	1.46E+00	2.72E-01	3.86E+01	3.86E+01	1.23E-05	SnO2	4.94E+01	1.57E-05	-	0		0
	116	6.36E+02	6.76E+00	5.06E-01	6.43E+02	6.43E+02	2.04E-04		8.20E+02	2.61E-04	-	0		0
	117	7.67E+02	3.47E+01	6.62E+00	8.08E+02	8.08E+02	2.57E-04		1.03E+03	3.27E-04	-	0		0
	118	8.05E+02	3.42E+01	6.48E+00	8.46E+02	8.46E+02	2.69E-04		1.08E+03	3.42E-04	-	0		0
	119	8.11E+02	3.42E+01	6.48E+00	8.52E+02	8.52E+02	2.71E-04		1.08E+03	3.43E-04	-	0		0
	120	8.02E+02	3.46E+01	6.59E+00	8.43E+02	8.43E+02	2.68E-04		1.07E+03	3.39E-04	-	0		0
	122	8.61E+02	3.82E+01	7.26E+00	9.06E+02	9.06E+02	2.88E-04		1.14E+03	3.63E-04	-	0		0
	124	1.20E+03	4.93E+01	9.29E+00	1.26E+03	1.26E+03	4.01E-04		1.59E+03	5.04E-04	-	0		0
	126	2.53E+03	8.03E+01	1.47E+01	2.62E+03	2.62E+03	8.32E-04		3.29E+03	1.04E-03	3.15E+12	2.20E-13	1.14E+00	0.000159
Sb	121	7.46E+02	3.52E+01	6.78E+00	7.88E+02	7.88E+02	2.50E-04	Sb2O3	9.44E+02	3.00E-04	-	0		0
	123	9.46E+02	4.22E+01	8.04E+00	9.96E+02	9.96E+02	3.16E-04		1.19E+03	3.78E-04	-	0		0
	125	3.52E+02	1.22E+01	2.38E+00	3.67E+02	3.67E+02	1.16E-04		4.37E+02	1.39E-04	8.74E+07	7.93E-09	0.5274	0.3753
Te	122	8.41E+01	8.46E-01	4.47E-02	8.50E+01	8.50E+01	2.70E-05	TeO2	1.07E+02	3.41E-05	-	0		0
	124	6.07E+01	6.27E-01	3.46E-02	6.14E+01	6.14E+01	1.95E-05		7.72E+01	2.45E-05	-	0		0
	125	1.39E+03	5.22E+01	9.55E+00	1.45E+03	1.45E+03	4.60E-04		1.82E+03	5.77E-04	-	0		0
	125	4.92E+00	1.71E-01	3.34E-02	5.13E+00	5.13E+00	1.63E-06		6.44E+00	2.05E-06	5.01E+06	1.38E-07	1.42E-01	0.0246
	126	1.98E+02	2.55E+00	3.09E-01	2.01E+02	2.01E+02	6.38E-05		2.52E+02	8.00E-05	-	0		0
	128	7.35E+03	2.08E+02	3.86E+01	7.59E+03	7.59E+03	2.41E-03		9.49E+03	3.02E-03	-	0		0
	130	2.09E+04	5.16E+02	9.43E+01	2.15E+04	2.15E+04	6.83E-03		2.68E+04	8.52E-03	-	0		0

I	129	1.17E+04	3.12E+02	5.72E+01	1.21E+04									0
Cs	133	5.45E+04	1.43E+03	2.70E+02	5.62E+04	5.62E+04	1.79E-02	Cs2O	5.96E+04	1.89E-02	-	0		0
	134	1.10E+03	5.64E+00	3.33E-01	1.11E+03	1.11E+03	3.52E-04		1.17E+03	3.73E-04	6.51E+07	1.07E-08	1.717	4.6493
	135	6.67E+04	1.52E+03	2.79E+02	6.85E+04	6.85E+04	2.18E-02		7.25E+04	2.30E-02	7.26E+13	9.55E-15	5.63E-02	8.345E-06
	137	5.03E+04	1.17E+03	2.18E+02	5.17E+04	5.17E+04	1.64E-02		5.47E+04	1.74E-02	9.47E+08	7.30E-10	1.87E-01	1.5764
Ba	134	6.10E+03	3.44E+01	1.99E+00	6.13E+03	6.13E+03	1.95E-03	BaO	6.87E+03	2.18E-03	-	0		0
	135	4.56E+01	6.65E-02	1.68E-03	4.56E+01	4.56E+01	1.45E-05		5.10E+01	1.62E-05	-	0		0
	136	2.27E+03	2.62E+01	3.09E+00	2.30E+03	2.30E+03	7.30E-04		2.57E+03	8.16E-04	-	0		0
	137	8.53E+03	2.00E+02	3.69E+01	8.77E+03	8.77E+03	2.79E-03		9.79E+03	3.11E-03	-	0		0
	138	5.91E+04	1.40E+03	2.62E+02	6.07E+04	6.07E+04	1.93E-02		6.78E+04	2.15E-02	-	0		0
La	139	5.47E+04	1.34E+03	2.54E+02	5.63E+04	5.63E+04	1.79E-02	La_2O_3	6.61E+04	2.10E-02	-	0		0
Ce	140	5.21E+04	1.26E+03	2.38E+02	5.35E+04	5.35E+04	1.70E-02	CeO_2	6.58E+04	2.09E-02	-	0		0
	142	4.68E+04	1.16E+03	2.21E+02	4.82E+04	4.82E+04	1.53E-02		5.90E+04	1.88E-02	3.31E+18	2.09E-19	0	0
	144	2.08E+02	5.22E+00	1.04E+00	2.14E+02	2.14E+02	6.80E-05		2.62E+02	8.31E-05	2.46E+07	2.82E-08	0.1119	0.14357
Pr	141	5.11E+04	1.26E+03	2.38E+02	5.26E+04	5.26E+04	1.67E-02	Pr_6O_{11}	6.36E+04	2.02E-02	-	0		0
Nd	142	2.29E+03	1.23E+01	6.76E-01	2.31E+03	2.31E+03	7.33E-04	Nd_2O_3	2.70E+03	8.57E-04	-	0		0
	143	1.62E+05	1.07E+03	2.10E+02	1.64E+05	1.64E+05	5.20E-02		1.91E+05	6.07E-02	-	0		0
	144	5.86E+04	9.87E+02	1.91E+02	5.98E+04	5.98E+04	1.90E-02		6.97E+04	2.22E-02	6.62E+22	1.05E-23	0	0
	145	2.97E+04	8.00E+02	1.55E+02	3.06E+04	3.06E+04	9.73E-03		3.57E+04	1.13E-02	-	0		0
	146	2.80E+04	7.08E+02	1.33E+02	2.88E+04	2.88E+04	9.15E-03		3.35E+04	1.07E-02	-	0		0
	148	1.73E+04	4.54E+02	8.52E+01	1.78E+04	1.78E+04	5.65E-03		2.07E+04	6.57E-03	-	0		0
	150	1.03E+04	2.66E+02	4.80E+01	1.06E+04	1.06E+04	3.38E-03		1.23E+04	3.92E-03	-	0		0
Pm	147	2.57E+03	9.05E+01	1.85E+01	2.68E+03	2.68E+03	8.52E-04	Pm_2O_3	3.12E+03	9.91E-04	8.28E+07	8.39E-09	6.05E-02	0.2833
Sm	147	1.13E+04	4.11E+02	8.31E+01	1.18E+04	1.18E+04	3.76E-03	Sm_2O_3	1.38E+04	4.37E-03	3.38E+18	2.05E-19	2.31	1.166E-09
	148	8.08E+03	5.63E+01	3.81E+00	8.14E+03	8.14E+03	2.59E-03		9.46E+03	3.00E-03	2.53E+23	2.74E-24	2.014	9.284E-15
	149	1.12E+04	3.25E+02	6.27E+01	1.16E+04	1.16E+04	3.69E-03		1.35E+04	4.29E-03	3.15E+23	2.20E-24	0	0
	150	4.10E+03	3.05E+01	1.67E+00	4.14E+03	4.14E+03	1.31E-03		4.80E+03	1.52E-03	-	0		0
	151	5.56E+03	1.69E+02	3.20E+01	5.76E+03	5.76E+03	1.83E-03		6.68E+03	2.12E-03	2.84E+09	2.44E-10	1.98E-02	0.00564
	152	9.55E+03	1.68E+02	2.63E+01	9.75E+03	9.75E+03	3.10E-03		1.13E+04	3.59E-03	-	0		0
	154	3.11E+03	6.52E+01	1.09E+01	3.18E+03	3.18E+03	1.01E-03		3.68E+03	1.17E-03	-	0		0
Eu	151	2.37E+02	8.61E+00	1.67E+00	2.47E+02	2.47E+02	7.86E-05	Eu_2O_3	2.87E+02	9.11E-05	-	0		0
	153	3.31E+03	9.08E+01	1.67E+01	3.42E+03	3.42E+03	1.09E-03		3.95E+03	1.26E-03	-	0		0
	154	8.77E+02	6.73E+00	3.74E-01	8.84E+02	8.84E+02	2.81E-04		1.02E+03	3.25E-04	2.71E+08	2.56E-09	1.51E+00	0.679151136
	155	8.16E+02	1.62E+01	2.79E+00	8.35E+02	8.35E+02	2.65E-04		9.64E+02	3.06E-04	1.57E+08	4.43E-09	0.1227	0.08960
Gd	152	1.27E+01	1.21E-01	9.90E-03	1.28E+01	1.28E+01	4.06E-06	Gd_2O_3	1.48E+01	4.70E-06	-	0.00E+00		0
	154	5.19E+02	4.24E+00	2.31E-01	5.24E+02	5.24E+02	1.66E-04		6.05E+02	1.92E-04	-	0		0
	155	1.07E+03	2.36E+01	4.08E+00	1.10E+03	1.10E+03	3.49E-04		1.27E+03	4.04E-04	-	0		0
	156	2.47E+03	3.32E+01	4.81E+00	2.51E+03	2.51E+03	7.96E-04		2.89E+03	9.18E-04	-	0		0

	157	6.56E+02	1.63E+01	2.99E+00	6.75E+02	6.75E+02	2.15E-04		7.79E+02	2.47E-04	-	0		0
	158	1.31E+03	1.58E+01	2.01E+00	1.33E+03	1.33E+03	4.21E-04		1.53E+03	4.85E-04	-	0		0
	160	2.35E+02	3.89E+00	5.95E-01	2.39E+02	2.39E+02	7.60E-05		2.75E+02	8.74E-05	-	0		0
Tb	159	3.67E+02	6.36E+00	1.01E+00	3.74E+02	3.74E+02	1.19E-04	Tb_2O_3	4.30E+02	1.37E-04	-	0		0
Dy	160	1.02E+02	4.90E-01	2.30E-02	1.03E+02	1.03E+02	3.27E-05	Dy_2O_3	1.18E+02	3.76E-05	-	0		0
	161	1.04E+02	1.73E+00	2.82E-01	1.06E+02	1.06E+02	3.35E-05		1.21E+02	3.85E-05	-	0		0
	162	9.83E+01	1.29E+00	1.82E-01	9.98E+01	9.98E+01	3.17E-05		1.15E+02	3.64E-05	-	0		0
	163	3.76E+01	5.54E-01	8.37E-02	3.83E+01	3.83E+01	1.22E-05		4.39E+01	1.39E-05	-	0		0
	164	2.11E+01	3.41E-01	5.06E-02	2.15E+01	2.15E+01	6.82E-06		2.46E+01	7.82E-06	-	0		0
U	234	2.00E+03	3.13E+00	6.03E-01	2.01E+03	2.01E+00	6.38E-07	U_3O_8	2.37E+00	7.54E-07	-	0		0
	235	7.38E+03	2.18E+04	2.46E+04	5.38E+04	5.38E+01	1.71E-05		6.36E+01	2.02E-05	2.22E+16	3.12E-17	4.42E+00	9.667E-10
	236	4.12E+03	1.56E+03	6.75E+02	6.35E+03	6.35E+00	2.02E-06		7.50E+00	2.38E-06	7.39E+14	9.38E-16	4.57E+00	3.530E-09
	238	6.95E+06	9.03E+06	8.90E+06	2.49E+07	2.49E+04	7.90E-03		2.93E+04	9.32E-03	1.41E+17	4.92E-18	4.28E+00	6.736E-08
Np	237	1.08E+04	5.40E+02	2.12E+02	1.15E+04	1.15E+01	3.65E-06	NpO_2	1.31E+01	4.15E-06	6.75E+13	1.03E-14	5.16E+00	7.894E-08
Pu	238	3.17E+04	4.75E+01	5.61E+00	3.18E+04	3.18E+01	1.01E-05	PuO_2	3.60E+01	1.15E-05	2.77E+09	2.50E-10	5.59E+00	0.00571
	239	1.09E+06	2.36E+05	9.16E+04	1.42E+06	1.42E+03	4.51E-04		1.61E+03	5.11E-04	7.59E+11	9.11E-13	5.20E+00	0.00086
	240	7.87E+05	8.15E+03	1.28E+03	7.96E+05	7.96E+02	2.53E-04		9.02E+02	2.87E-04	2.06E+11	3.35E-12	5.25E+00	0.00178
	241	9.65E+04	1.37E+02	9.72E+00	9.66E+04	9.66E+01	3.07E-05		1.09E+02	3.48E-05	4.54E+08	1.53E-09	5.23E-03	9.816E-05
	242	9.24E+04	2.45E+00	7.38E-02	9.24E+04	9.24E+01	2.93E-05		1.05E+02	3.32E-05	1.22E+13	5.68E-14	6.66E-02	0.000112
Am	241	5.83E+04	4.39E+01	3.23E+00	5.83E+04	5.83E+01	1.85E-05	Am_2O_3	6.42E+01	2.04E-05	1.36E+10	5.08E-11	5.60E+00	0.0021080
	242	2.11E+03	2.83E-02	6.82E-04	2.11E+03	2.11E+00	6.72E-07		2.32E+00	7.38E-07	4.80E+09	1.45E-10	6.66E-02	2.582E-06
	243	3.37E+04	3.85E-02	5.03E-04	3.37E+04	3.37E+01	1.07E-05		3.71E+01	1.18E-05	2.33E+11	2.98E-12	5.42E+00	6.859E-05
Cm	242	1.07E+01	3.03E-04	8.56E-06	1.07E+01	1.07E-02	3.39E-09	Cm_2O_3	1.17E-02	3.73E-09	1.41E+07	4.92E-08	6.22E+00	0.000413
	243	2.00E+02	9.51E-04	9.37E-06	2.00E+02	2.00E-01	6.34E-08		2.19E-01	6.96E-08	8.99E+08	7.71E-10	6.19E+00	0.0001199
	244	1.86E+04	7.66E-04	3.47E-06	1.86E+04	1.86E+01	5.90E-06		2.04E+01	6.48E-06	5.72E+08	1.21E-09	5.90E+00	0.0166383
	245	4.82E+03	1.23E-05	1.95E-08	4.82E+03	4.82E+00	1.53E-06		5.30E+00	1.68E-06	2.68E+11	2.59E-12	5.60E+00	8.740E-06
	246	4.32E+02	5.33E-08	2.86E-11	4.32E+02	4.32E-01	1.37E-07		4.74E-01	1.51E-07	1.49E+11	4.65E-12	5.52E+00	1.380E-06
	247	1.44E+01	1.79E-10	3.08E-14	1.44E+01	1.44E-02	4.57E-09		1.58E-02	5.02E-09	4.92E+14	1.41E-15	5.35E+00	1.344E-11
Total (FP+Ac)		1.07E+07	9.33E+06	9.03E+06	2.91E+07	1.61E+06	5.12E-01		1.98E+06	6.29E-01				1.14E+01
Na	23	2.40E+05	2.08E+05	2.01E+05	6.49E+05	6.49E+05	2.06E-01	Na_2O	8.75E+05	2.78E-01				
P	30.97	4.22E+03	3.67E+03	3.55E+03	1.14E+04	1.14E+04	3.63E-03	P_2O_5	3.21E+04	1.02E-02				
Fe	55.85	4.51E+04	3.92E+04	3.79E+04	1.22E+05	1.22E+05	3.88E-02	Fe_2O_3	1.75E+05	5.55E-02				
Ni	58.69	1.18E+04	1.03E+04	9.93E+03	3.20E+04	3.20E+04	1.02E-02	NiO	4.07E+04	1.29E-02				
Cr	52	1.17E+04	1.02E+04	9.84E+03	3.17E+04	3.17E+04	1.01E-02	Cr_2O_3	4.64E+04	1.47E-02				
Oxygen						6.88E+05	2.19E-01							
Total						3.15E+06	1.00E+00		3.15E+06	1.00E+00				

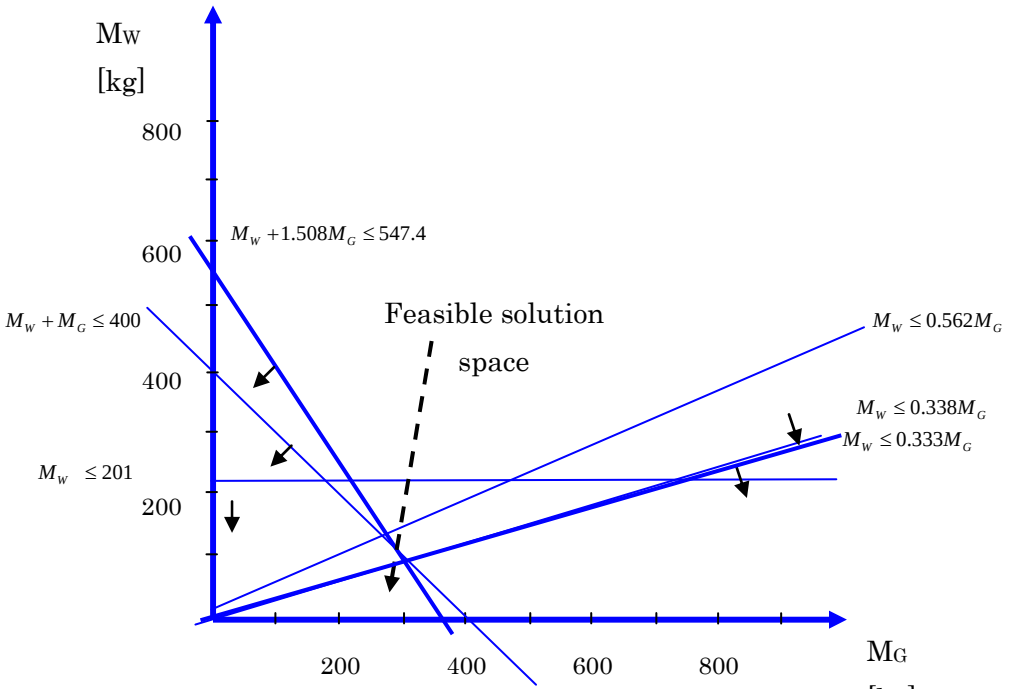

Figure 5: Graphical solution for optimum FBR-HLW conditioning

V.3 Mass Loadings of Selected Radionuclides in HLW Canister

From the results shown in Table III and Table V, the values of the mass loadings $\hat{M}^o$ per canister for important radionuclides in the solidified HLW from LWR and FBR spent fuels have been obtained as shown in Table VI.

In Table III, mass of each radionuclide per MT of PWR spent fuel is tabulated. With the value, 0.79 canister/MT, the value for the number, *m*, of moles per canister has been calculated as, for *x* g/MT, $m = x/0.79/M_A$, where M_A is the molecular mass. For example, for Am-243, $x = 21.71$ g. Therefore, $m = 21.71/0.79/243 = 0.113$ mol/canister (see Table VI).

In Table V, mass of each radionuclide for 29.1 MTHM of spent fuel is tabulated. 1.09 canister/MTHM has been obtained. Therefore, the mass shown in Table V for each radionuclide is stored in 1.09 x 29.1 = 31.7 canisters. For *x* g shown in Table V, the value for the number, *m*, of moles per canister has been calculated as $m = x/31.7/M_A$. For example, for Am-243, $x = 33.7$ g. Therefore, $m = 33.7/31.7/243 = 4.37\text{E-}3$ mol/canister.

In Table VI, numbers of moles of selected radionuclides in a single canister are summarized. Mass loadings of precursors to ^{237}Np, ^{240}Pu, ^{242}Pu, and ^{239}Pu are lumped with mass loadings of their short-lived precursors because the precursors decay to them by the time the

canisters fail in a geologic repository. These lumped values are also shown in Table VI, and used for the environmental impact calculation.

Table VI: Mass Loadings of Important Radionuclides in a Canister of Solidified HLW and Their Parameter Values for Environmental Impact Evaluations.

Nuclide	$\hat{M}^o$ (mol/canister)				MPC (Ci/m^3) [14]	$\hat{\lambda}$ (1/s)	Conversion factor $\hat{C}$ (m^3/kg)
	PWR		FBR				
		Lumped		Lumped			
Cm 247	0		1.84E-6				
Pu 243	0		0				
Am 243	1.13E-1		4.37E-3				
Pu 239	8.10E-2	**1.94E-1**	1.88E-1	**1.92E-1**	2.00E-8	9.11E-13	3.1E+9
Cm 244	2.82E-2		2.40E-3				
Pu 240	3.32E-2	**6.14E-2**	1.05E-1	**1.07E-1**	2.00E-8	3.35E-12	1.1E+10
Cm 246	6.69E-5		5.54E-5				
Am 242m	1.75E-3		2.75E-4				
Pu 242	2.79E-3	**4.61E-3**	1.20E-2	**1.24E-2**	2.00E-8	5.68E-14	1.9E+8
Cm 245	9.14E-4		6.21E-4				
Pu 241	1.01E-2		1.26E-2				
Am 241	2.04E-1		7.63E-3				
Np 237	2.02E+0	**2.24E+0**	1.53E-3	**2.24E-2**	2.00E-8	1.03E-14	3.5E+7
I 129	**1.40E+0**		**2.96E+0**		2.00E-7	4.30E-8	8.60E+5
Cs 135	**2.75E+0**		**1.60E+1**		1.00E-5	3.01E-7	1.15E+5
Tc 99	**9.33E+0**		**1.20E+1**		6.00E-5	3.28E-6	2.85E+5
Se 79	**8.09E-2**		**1.04E-1**		8.00E-6	3.38E-13	8.70E+6
Zr 93	**9.02E+0**		**8.58E+0**		4.00E-5	1.44E-14	6.30E+4
Pd 107	**1.69E+0**		**6.34E+0**		5.00E-4	3.38E-15	1.03E+3
Sn 126	**1.12E-1**		**6.56E-1**		5.00E-7	2.20E-13	7.10E+6

Iodine will not be included in the HLW canister in reality. In the present study, hypothetically, ^{129}I is also included in the HLW canister, and is assumed to be released congruently with waste matrix dissolution.

Pu, Np, Tc, Se, Zr, Pd, and Sn are considered to be released with the solubility-limited mode. Cs is assumed to be released congruently with the waste matrix. For congruent release, the waste-matrix dissolution time is assumed to be 50,000 years. Other parameter values related to repository design have been taken from [8].

Contribution of other radionuclides to environmental impact is not significant, compared to those listed in Table VI, because of (1) too long half-lives, (2) too short half-lives, (3) large MPC, and/or (4) small mass loading in a canister.

To judge the importance of radionuclides in terms of contribution to the environmental impact, the quantity $\hat{M}^o \hat{C} \exp\left(-\hat{\lambda} t\right)$ has bee evaluated for each radionuclide, where *t* is set to be 50,000 years to take into account the delay of release into the environment due to dissolution of waste matrix. Those radionuclides that have a value for the quantity significantly greater than 1E+4 m^3 are included in Table VI.

V.4 Parameter Values for Radionuclide Release and Transport

Based on the initial mass loadings per canister for PWR and FBR, the environmental impact from a repository containing 40,000 canisters of identical loadings has been numerically evaluated. Repository configuration and layout developed for the H12 study by JNC [8] have been applied. The values of $\hat{M}_i^o$ are also fixed as shown in Table VI.

Parameter values related to radionuclide transport in the buffer and in the near-field rock are summarized in Table VII. Geochemical parameters for radionuclide transport are summarized in Table VIII. Those include the solubility and the sorption distribution coefficients. The retardation factors are obtained by

$$K = 1 + \frac{1-\varepsilon}{\varepsilon} \rho K_{dB},\ R = 1 + \frac{1-\varepsilon_p}{\varepsilon_p} \rho_p K_{dR} \tag{28}$$

For an element including multiple isotopes, solubility sharing should be considered. For example, there are three major isotopes of Pu in the present calculation, for which Pu solubility should be allocated, proportional to the mass of each isotope in Pu precipitate. In the present assessment, however, the elemental solubility is assumed for all isotopes. This results in overestimate of the environmental impact.

In Table IX, based on the values of the aforementioned physical parameters, values for non-dimensionalized parameters are shown for radionuclides under the solubility-limited release mode. In Table X, values for non-dimensionalized parameters for congruently-released radionuclides are tabulated.

Numerical evaluation for environmental impact based on the formulation shown in Chapter 2 have been made by using these parameter values.

We first evaluate the environmental impact for the case where all parameter values have their central values. Effects of uncertainty associated with parameters are considered in Sec. V.7.

Table VII: Values of Transport Parameter Assumed for Environmental Impact Assessment, Based on H-12 Repository Design

Diffusion coefficient in the buffer, $\hat{D}$	0.03	m^2/yr
Flow rate of groundwater through a row of compartments, $\hat{F}$	0.45	m^3/yr
Porosity of the buffer, ε	0.3	
Porosity of the near-field rock, ε_p	0.5	
Density of the buffer, ρ	2100	kg/m^3
Density of the near-field rock, ρ_p	2600	kg/m^3
Pore velocity of groundwater in the near-field rock, $\hat{v}$	1	m/yr
Interfacial area between the waste form and the buffer, $\hat{S}$	1.81	m^2/yr
Distance between two adjacent waste forms, $\hat{d}$	10	m
Thickness of the buffer, $\hat{L}$	0.98	m
Volume of the near-field rock in a compartment, $\hat{V}$	9.05	m^3
Dissolution time of the waste matrix, $\hat{T}_L$	50,000	yr
Total number of canisters, $N_x N_y$	40,000	

Table VIII: Values for Geochemical Parameters for Environmental Impact Assessment, Based on Those Assumed for H-12 Repository Performance Assessment [8]

Nuclide	Solubility, $\hat{C}^*$ (mol/m^3)	Sorption distribution coefficient, (m^3/kg)		Retardation factor	
		In buffer, K_{dB}	In NFR, K_{dR}	in buffer, K	in NFR, R
Pu	1.0E-5	10	1	49000	2600
Np	2.0E-5	1	1	4900	2600
Tc	3.9E-5	0.1	1	490	2600
Se	3.0E-6	0	0.01	1	27
Zr	1.0E-3	10	0.1	49000	261
Pd	1.0E-6	0.1	0.1	491	261
Sn	5.0E-3	1	1	4900	2600
I	---	4E-5	0.003	1.2	8.7
Cs	---	0.01	0.05	50	131

Table IX: Values of Non-Dimensionalized Parameters for Radionuclides Released Under Solubility-Limited Release Mode

	α	μ	λ'	κ	β	ζ	γ	σ		T	
								LWR	FBR	LWR	FBR
Np-237	1.67E-01	2.22E-01	8.37E-03	2.24E-01	1.65E-01	4.59E-02	9.56E-01	2.33E-02	2.33E+00	2.85E+02	2.64E+00
Pu-240	1.67E-02	2.22E+00	2.78E+00	1.29E+01	1.07E-06	3.25E+00	2.35E-01	4.25E+00	2.44E+00	4.79E+00	4.99E+00
Pu-242			4.68E-02	1.68E+00	1.08E-02	1.13E-01	8.98E-01	5.66E+01	2.10E+01	1.18E+00	3.18E+00
Pu-239			7.43E-01	6.67E+00	2.81E-04	9.89E-01	5.03E-01	1.34E+00	1.36E+00	1.02E+01	1.02E+01
Se-79	8.48E+00	4.36E-03	2.90E-03	1.85E-02	8.48E+00	3.98E-02	9.62E-01	1.97E-05	1.54E-05	1.89E+03	5.96E+01
Zr-93	1.67E-03	2.21E+01	1.21E-03	8.51E-01	1.49E-03	4.67E-02	9.55E-01	2.89E+00	3.04E+00	5.15E+02	4.93E+02
Pd-107	1.67E-01	2.21E-01	2.80E-04	4.09E-02	1.67E-01	3.72E-02	9.64E-01	1.55E-04	4.12E-05	2.56E+04	3.03E+04
Sn-126	1.67E-01	2.22E-01	2.79E-03	1.29E-01	1.66E-01	3.99E-02	9.62E-01	1.16E+02	1.99E+01	5.14E-02	3.01E-01
Tc-99	1.66E+00	2.22E-02	8.58E-02	2.27E-01	1.65E+00	1.23E-01	8.90E-01	1.09E-03	9.70E-04	4.92E+01	5.06E+01

Table X: Values of Non-Dimensionalized Parameters for Congruently-Released Radionuclides

	T_L	λ
I-129	565.5392	3.9E-06
Cs-135	36.52835	0.000413

V.5 Results for Environmental Impact Evaluation

Figure 6 shows the numerical results for the relationship between the environmental impact from individual radionuclides included in the HLW canister for the PWR case and for the FBR case, as a function of the number of canisters connected in a row.

In both figures, for all radionuclides, it is observed that environmental impact decreases as more canisters are connected in a water stream. This is because as more canisters included in the same water stream, the residence time of the radionuclide in the repository becomes greater, resulting in greater loss by radioactive decay while it is in the repository.

For the PWR case, impact of ^{237}Np is the highest. The second highest contributor, ^{129}I, is about a factor of 20 smaller than that of ^{237}Np. Within the range between 1E+9 and 1E+10 m^3, impact from long-lived fission-product nuclides, such as ^{129}I, ^{126}Sn, ^{135}Cs, ^{93}Zr, are observed to be significant. Among Pu isotopes, contributions of ^{242}Pu and ^{239}Pu are also in the same range. The contribution of ^{240}Pu is significantly small, compared with the other Pu isotopes, because of the shortest half-life.

For the FBR case, the highest contributors are fission-product nuclides, i.e., ^{126}Sn, ^{129}I, ^{135}Cs, and ^{93}Zr. Impact of ^{237}Np is significantly smaller than that for the PWR case, and about the same level as that from those long-lived FPs. This results from the assumption that 99.9% of actinide elements, including Np, AM, and Cm (minor actinides), is recovered by the separation process for the FBR, whereas for the PWR case, no recovery is assumed for Np, Am, and Cm.

For the PWR case, if ^{237}Np and its decay precursors (^{245}Cm, ^{241}Pu, ^{241}Am) are removed from the HLW canister, the environmental impact of the repository can significantly and effectively reduced. For the FBR case, however, further removal of minor actinide would not reduce the repository impact significantly, because the repository impact is mainly determined by the long-lived FP nuclides included in the canisters. In this regard, the assumed recovery ratio, 99.9%, for the FBR case seems to aim at a reasonable level of separation.

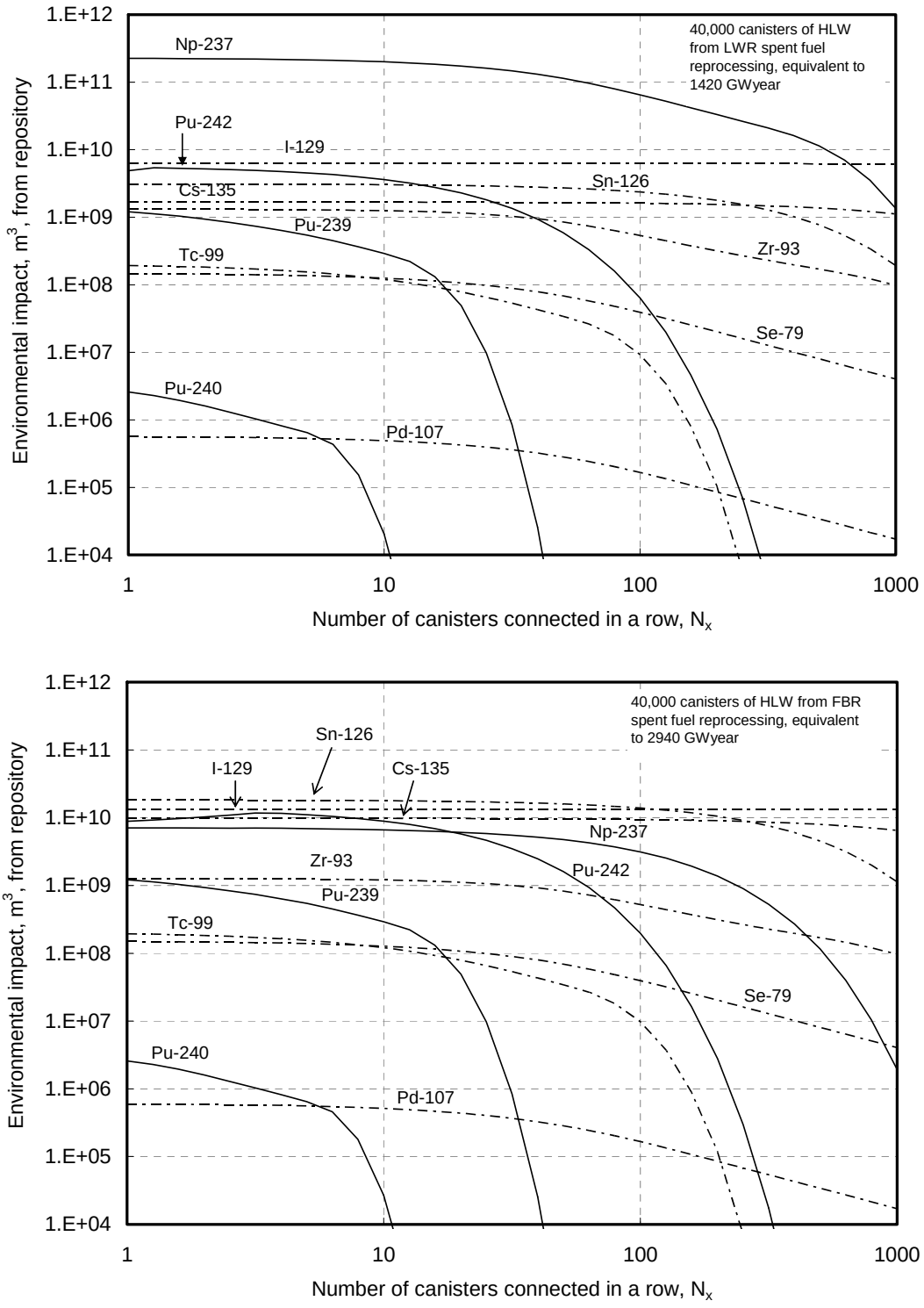

Figure 6 : Environmental impact from a repository containing 40,000 canisters as a function of the number of canisters connected in the same water flow stream. The left and right figures show the cases for LWR and FBR, respectively. The solid curves represent actinide radionuclides, whereas the dashed curves FP radionuclides.

V.6 Effects of Mass Loading in HLW Canister on Environmental Impact

Figure 7 shows the effects of mass loadings of Pu and Np on the environmental impact of the repository. As the mass loading of Np decreases, the environmental impact from this radionuclide decreases significantly. The environmental impact of Pu isotopes, however, is not sensitive to its initial mass loading. This is because transport of Pu in the repository is so slow with the parameter values assumed for this case that most of Pu isotopes decay before released from the edge of the repository to the environment. This observation would be different if greater mobility is assumed for Pu, for such mechanism as colloid-facilitated transport.

In this context, the FBR system is justified because it reduces mass loading of ^{237}Np and its decay precursors in a HLW canister, whose environmental impact is most sensitive to reduction of mass loading.

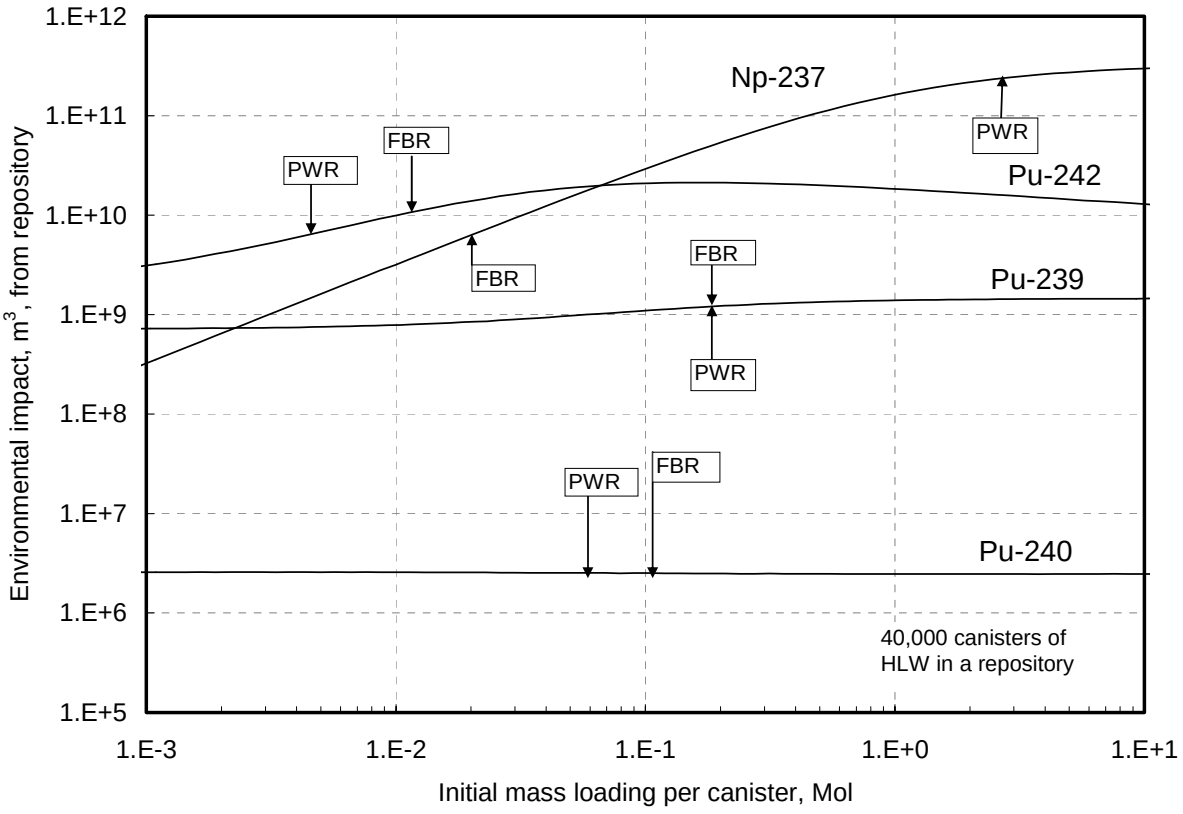

Figure 7: Effects of reduction in initial mass loadings per canister on the environmental impact from a 40,000-canister repository due to ^{237}Np, ^{242}Pu ^{240}Pu, and ^{239}Pu. Nx = 1 is assumed. For each curve, the mass loadings shown in Table VI for the PWR and FBR cases are indicated by arrows.

V.7 Bounding Analysis for Uncertainty with Transport Parameters

In the present evaluation, many parameters are included, which are subject to parameter uncertainties. In this section, we try to make a bounding analysis to find upper and lower bounds of the environmental impact of each radionuclide.

To simplify the present analysis, we assume that only parameters for radionuclide transport in a repository are subject to uncertainty. We assume that the repository design is fixed; the parameters for the engineered-barrier dimensions are considered fixed. Therefore, the values for those listed in Table VII, except for the dissolution time of the waste matrix, are fixed at the values shown in the table. For the dissolution time, we assume that it ranges between 5,000 and 500,000 years with 50,000 years as the central value.

Among the geochemical parameters whose values are listed in Table VIII, we assume that the solubility and sorption distribution coefficients vary in two orders of magnitude with the values in Table VIII as the central value. For example, the solubility of Pu is assumed to vary between 1.0E-6 to 1.0E-4 mol/m^3 with 1.0E-5 mol/m^3 as the median. For the sorption distribution coefficients, also two orders of magnitude range is assumed for each element.

Because the chemical behavior in the EBS and in the host rock around the EBS should be similar for the same element, it is assumed that when the distribution coefficient in the buffer takes its lower bound value, that in the NFR takes also its lower bound value. For example, for Pu, in the buffer, the coefficient ranges between 1 and 100 m^3/kg, and in the NFR between 0.1 and 10 m^3/kg. When the coefficient in the buffer is 1 m^3/kg, the coefficient in the NFR should be 0.1 m^3/kg. See Table XI for solubility-limited elements and Table XIII for congruent-release elements.

If we set the ranges of the physical parameters as mentioned above, the ranges of the non-dimensionalized parameters can be determined. The numerical results are shown in Table XII for solubility-limited nuclides and in Table XIV for congruent-release nuclides. In Table XII, it is observed for solubility-limited radionuclides that α and μ are almost invariant. λ' is proportional to the sorption distribution coefficients. In Table XIV, ranges of two fundamental non-dimensionalized parameters are shown. For these, combinations of ranges of the dissolution time $\hat{T}_L$ and the sorption distribution coefficients have been set in such a way that the intervals of the non-dimensionalized parameters become the widest.

Table XI: Uncertainty Ranges for Solubility Limited Radionuclides for N_x = 1.

Nuclide	Solubility, $\hat{C}^*$ (mol/m^3)			Sorption distribution coefficient, (m^3/kg) In buffer, K_{dB}			In NFR, K_{dR}		
	Lower	Median	Upper	Lower	Median	Upper	Lower	Median	Upper
Pu	1.0E-6	1.0E-5	1.0E-4	1	10	100	0.1	1	10
Np	2.0E-6	2.0E-5	2.0E-4	0.1	1	10	0.1	1	10
Tc	3.9E-6	3.9E-5	3.9E-4	0.01	0.1	1	0.1	1	10
Se	3.0E-7	3.0E-6	3.0E-5	0	0	0	0.001	0.01	0.1
Zr	1.0E-4	1.0E-3	1.0E-2	1	10	100	0.01	0.1	1
Pd	1.0E-7	1.0E-6	1.0E-5	0.01	0.1	1	0.01	0.1	1
Sn	5.0E-4	5.0E-3	5.0E-2	0.1	1	10	0.1	1	10

Table XII: Ranges of Environmental Impact for Solubility-Limited Nuclides Resulting From Uncertainties Associated with Non-Dimensionalized Parameters

		μ	α	λ'	σ		P		Environmental impact, m^3	
					PWR	FBR	PWR	FBR	PWR	FBR
Np-237	Lower Bound	2.21E-01	1.67E-01	8.40E-04	2.33E-04	2.33E-02	4.28E-02	8.15E-01	3.20E+10	6.09E+09
	Median	2.22E-01	1.67E-01	8.37E-03	2.33E-02	2.33E+00	3.02E-01	9.42E-01	2.26E+11	7.04E+09
	Upper Bound	2.22E-01	1.67E-01	8.37E-02	2.33E+00	2.33E+02	6.25E-01	8.57E-01	4.67E+11	6.41E+09
Pu-240	Lower Bound	2.21E+00	1.67E-02	2.79E-01	4.25E-02	2.44E-02	2.44E-04	1.41E-04	1.58E+09	1.59E+09
	Median	2.22E+00	1.67E-02	2.78E+00	4.25E+00	2.44E+00	4.00E-07	2.29E-07	2.59E+06	2.58E+06
	Upper Bound	2.22E+00	1.67E-02	2.78E+01	4.25E+02	2.44E+02	1.36E-18	7.79E-19	8.82E-06	8.80E-06
Pu-242	Lower Bound	2.21E+00	1.67E-02	4.70E-03	5.66E-01	2.10E-01	5.87E-01	3.80E-01	4.98E+09	8.67E+09
	Median	2.22E+00	1.67E-02	4.68E-02	5.66E+01	2.10E+01	5.86E-01	3.92E-01	4.97E+09	8.94E+09
	Upper Bound	2.22E+00	1.67E-02	4.68E-01	5.66E+03	2.10E+03	4.57E-01	4.16E-01	3.87E+09	9.49E+09
Pu-239	Lower Bound	2.21E+00	1.67E-02	7.45E-02	1.34E-02	1.36E-02	1.35E-03	1.36E-03	7.69E+09	7.66E+09
	Median	2.22E+00	1.67E-02	7.43E-01	1.34E+00	1.36E+00	2.13E-04	2.15E-04	1.21E+09	1.21E+09
	Upper Bound	2.22E+00	1.67E-02	7.43E+00	1.34E+02	1.36E+02	1.06E-09	1.08E-09	6.04E+03	6.09E+03
Se-79	Lower Bound	3.27E-02	1.13E+00	3.86E-04	1.97E-06	1.54E-06	5.53E-03	4.33E-03	1.23E+07	1.24E+07
	Median	4.36E-03	8.48E+00	2.90E-03	1.97E-05	1.54E-05	5.26E-02	4.16E-02	1.47E+08	1.49E+08
	Upper Bound	4.51E-04	8.20E+01	2.80E-02	1.97E-04	1.54E-04	3.46E-01	2.94E-01	7.70E+08	8.41E+08
Zr-93	Lower Bound	2.13E+01	1.73E-03	1.25E-04	2.89E-02	3.04E-02	2.73E-01	2.83E-01	5.77E+08	6.06E+08
	Median	2.21E+01	1.67E-03	1.21E-03	2.89E+00	3.04E+00	5.84E-01	5.89E-01	1.23E+09	1.26E+09
	Upper Bound	2.22E+01	1.67E-03	1.21E-02	2.89E+02	3.04E+02	2.44E-01	2.50E-01	5.16E+08	5.35E+08
Pd-107	Lower Bound	2.18E-01	1.70E-01	2.90E-05	1.57E-06	4.20E-07	8.80E-03	2.37E-03	6.56E+04	6.13E+04
	Median	2.21E-01	1.67E-01	2.80E-04	1.55E-04	4.12E-05	8.18E-02	2.31E-02	5.64E+05	5.97E+05
	Upper Bound	2.22E-01	1.67E-01	2.79E-03	1.54E-02	4.11E-03	4.66E-01	1.90E-01	3.47E+06	4.91E+06
Sn-126	Lower Bound	2.21E-01	1.67E-01	2.80E-04	1.17E+00	1.99E-01	9.96E-01	9.90E-01	3.99E+09	2.32E+10
	Median	2.22E-01	1.67E-01	2.79E-03	1.16E+02	1.99E+01	9.89E-01	9.89E-01	3.96E+09	2.32E+10
	Upper Bound	2.22E-01	1.67E-01	2.79E-02	1.16E+04	1.99E+03	9.30E-01	9.30E-01	3.73E+09	2.18E+10
Tc-99	Lower Bound	2.25E-02	1.64E+00	8.61E-03	1.11E-05	9.88E-06	2.02E-03	1.80E-03	2.13E+07	2.13E+07
	Median	2.22E-02	1.66E+00	8.58E-02	1.09E-03	9.70E-04	1.83E-02	1.63E-02	1.93E+08	1.93E+08
	Upper Bound	2.22E-02	1.67E+00	8.58E-01	1.09E-01	9.69E-02	7.98E-02	7.26E-02	8.40E+08	8.60E+08

In Table XII, numerical results for the bounding analysis are shown. Environmental impact of each nuclide for the lower- and upper bounds and the central values are shown. While each geochemical parameters is assumed to have two orders of magnitude variation, variations observed for ^{237}Np, ^{242}Pu, ^{79}Se, ^{93}Zr, ^{126}Sn, and ^{99}Tc are smaller than two orders of magnitude. For ^{240}Pu and ^{239}Pu, effects of parameter variations are significant.

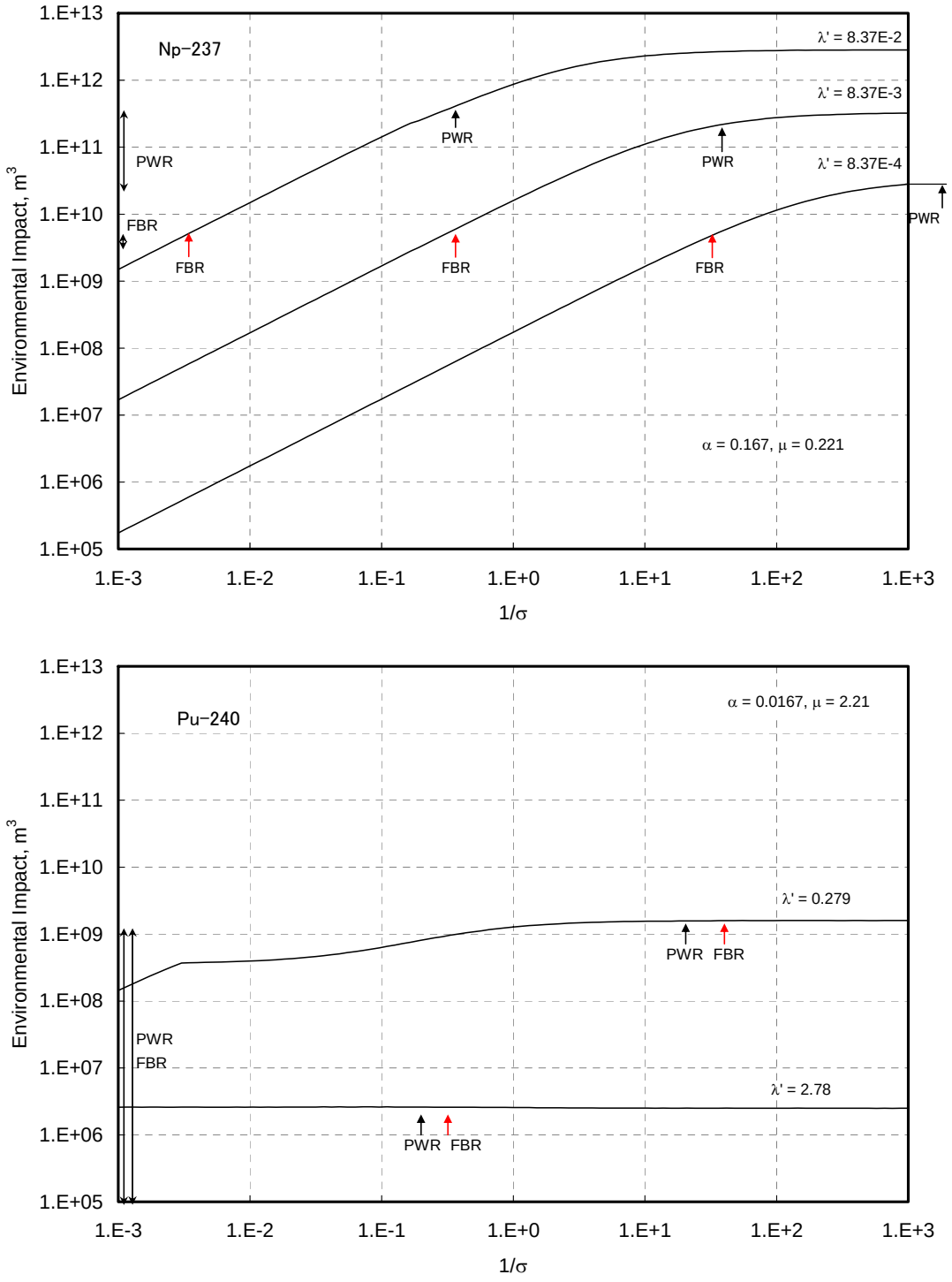

Figure 8: Effects of non-dimensionalized parameters on environmental impact of ^{237}Np and ^{240}Pu. Long-lived FP shows similar tendency as ^{237}Np. For ^{240}Pu, the lower bound curve is far below. The arrows close to the left axis show the uncertainty ranges for the environmental impact.

For these long-lived radionuclides (^{237}Np, ^{242}Pu, ^{79}Se, ^{93}Zr, ^{126}Sn, and ^{99}Tc), regardless of mobility of radionuclides in the repository, most of the mass loaded initially in the waste canister will survive the transport in the repository, and eventually be released to the environment. For relatively short-lived radionuclides, such as ^{240}Pu and ^{239}Pu, effects of geochemical parameters are important because the residence time in the repository could become shorter or longer than the decay lifetime. If the decay lifetime is longer than the residence time, then the environmental impact would become great. This is observed in the lower bound case for ^{240}Pu and ^{239}Pu.

For all radionuclide observed in Table XII, similar observations can be made for the PWR case and for the FBR case. For ^{237}Np, as observed in Figure 8, uncertainty for the PWR case is about 1 order of magnitude while that for FBR is negligibly small. Because the mass loading in a waste canister for the FBR case is about two orders of magnitude smaller, than that for the PWR case, decay loss of ^{237}Np in the repository region is significant, relative to that released to the environment.

This can be claimed as an advantage of the FBR system, if compared with the PWR system. With the HLW from PWR in the repository, the repository impact would become more than 20 times greater than that from FBR case, with greater uncertainty. By applying the FBR system, the environmental impact can be reduced, and the impact can be evaluated with greater certainty.

Table XIII：Uncertainty Ranges for Congruent-Release Radionuclides for N_x = 1.

Nuclide	Dissolution time of waste matrix, $\hat{T}_L$, yr			Sorption distribution coefficient, (m^3/kg) In buffer, K_{dB}			In NFR, K_{dR}		
	Lower	Median	Upper	Lower	Median	Upper	Lower	Median	Upper
I	500,000	50,000	5,000	0	4E-5	4E-4	0	0.003	0.03
Cs				0.001	0.01	0.1	0.005	0.05	0.5

Table XIV: Ranges of Environmental Impact for Congruent-Release Nuclides Resulting From Uncertainties Associated with Non-Dimensionalized Parameters

		T_L	λ	P	Environmental Impact, m^3	
					PWR	FBR
I-129	Lower Bound	4.47E+04	4.93E-07	9.78E-01	6.08E+09	1.28E+10
	Median	5.65E+02	3.90E-06	9.98E-01	6.20E+09	1.31E+10
	Upper Bound	6.39E+00	3.46E-05	9.997E-01	6.21E+09	1.31E+10
Cs-135	Lower Bound	3.40E+03	4.43E-05	8.60E-01	1.47E+09	8.55E+09
	Median	3.6E+01	4.13E-04	9.85E-01	1.68E+09	9.78E+09
	Upper Bound	3.68E-01	4.09E-03	9.95E-01	1.70E+09	9.88E+09

In Table XIV, numerical results for the bounding analysis for congruent-release nuclides are shown. Variations of the environmental impact for ^{129}I and ^{135}Cs are small (within one order of magnitude).

Thus, after having performed the bounding analysis, it can be said that the most important contributors to the environmental impact for the FBR system are long-lived fission products, ^{129}I, ^{126}Sn, and ^{135}Cs. Among actinide nuclides, ^{237}Np and ^{242}Pu are important contributors, but not more than those long-lived FP nuclides. If the repository conditions become unfavorable to confinement, contributions of short-lived Pu isotopes, ^{239}Pu and ^{240}Pu can be important, but these will not affect the total impact significantly. The environmental impact from the 40,000-canister repository for the FBR is likely to be 2.3E10 m^3 for N_x = 1.

For the PWR case, from Table XII and Figure 8, the environmental impact from the 40,000-canister repository ranges between 3.2E10 and 4.7E11 m^3. We choose 2.5E11 m^3 as the central value.

V.8 Advantages of FBR

If we do not deploy any new system and keep utilizing the present fleet of PWRs, the rate of increase of the environmental impact from the repository is 1.7E8 m^3 per GW·yr.[7]

If we deploy a fuel cycle with the FBR considered here, the impact is primarily due to ^{126}Sn as observed in Figure 6, and the rate of increase of the impact is similarly calculated as 2.3E10 m^3/2,940 GW·yr = 7.8E6 m^3/GWyr. Thus, the impact of PWR is 22 times greater than that from FBR for the same amount of electricity generation.

As we observed in the previous section, with HLW from FBR, the uncertainty associated with the environmental impact due to parameter uncertainties with transport parameters becomes smaller than that with HLW from PWR.

While the aforementioned advantages are considered primarily those resulting from high recovery efficiency of the separation process, there is additional advantage that is directly related to the FBR utilization. With the FBR system, roughly 1 ton of depleted uranium is *consumed* per GW·yr. One ton of depleted uranium is equivalent to 5.3E7 m^3 of impact. By deploying the FBR

[7] This can be obtained by dividing the impact, 2.45E11 m^3, from ^{237}Np by the total electricity generation, 1420 GW·yr, for the 40,000-canister repository with identical canisters from PWR spent fuel.

system, depleted uranium is converted to the HLW which causes 7.8E6 m^3/GWyr of impact. Thus, as far as depleted uranium supply lasts, the net rate of *decrease* of the total impact can be achieved by deploying the FBR system.

Because of the significant difference between the impact per unit electricity generation between PWR and FBR, transition from the present PWR system to the FBR system with high recovery efficiencies for actinide elements is highly recommended. The sooner and the faster the transition is, the longer the repository availability will be.

VI. CONCLUSIONS

Environmental impacts from the HLW geologic repository containing 40,000 canisters have been quantitatively evaluated for LWR and FBR. The waste-conditioning model that determines the composition of the solidified HLW and the number of canisters per unit mass of spent fuel has been applied. Mathematical formulae for the peak mass of radionuclides that exist in the environment after released from the repository have been derived. With these mathematical developments, the environmental impact of the repository has been formulated in terms of the repository-design parameters and the isotope vector of the high-level liquid waste from the fuel cycle. Uncertainty has been investigated by performing a bounding analysis to consider ranges for geochemical parameters that affect release and transport of nuclides in the repository.

With the developed formulae, the environmental impact from the repository with HLW from PWR operation and from FBR operation has been numerically obtained. From the numerical results, the following observations have been made.

- In the HLW from PWR spent fuel, ^{237}Np including its decay precursors are the major sources of environmental impact. The reduction of these nuclides would be meaningful until the environmental impact of ^{237}Np is reduced to the level of environmental impacts of dominating FP nuclides, such as ^{129}I and ^{135}Cs.
- The environmental impact from a FBR-HLW repository is smaller than that from the FBR repository by a factor of 10. If compared on a per GWyr basis, the advantage of FBR is even greater (a factor of 20).
- Uncertainty associated with the environmental impact can become smaller with the FBR HLW than with PWR HLW.
- The possibility of decreasing the environmental impact from the entire cycle, including legacy depleted uranium, by deployment of the FBR system has been indicated.
- ^{129}I could be one of the major contributor of the environmental impact because of its long half life and inert behavior in geologic environment. In this analysis, effects of ^{129}I has been studied by adding hypothetical mass loading into a HLW canister.

VII. REFERENCES

[1] Ahn, J., D. Kawasaki, P. L. Chambré, Relationship among Performance of Geologic Repositories, Canister-Array Configuration, and Radionuclide Mass in Waste, *Nuclear Technology*, **126**, 94-112, 2002.

[2] Ahn, J., An Environmental Impact Measure for Nuclear Fuel Cycle Evaluation, *Journal of Nuclear Science and Technology*, **41**(3), 296-306, 2004.

[3] Ahn, J., Environmental Impact of Yucca Mountain Repository, this Proceedings.

[4] Cheon, M., and J. Ahn, Linear Programming Approach for Modeling Solidification of HLW from ATW Fuel Cycle, this Proceedings

[5] Benedict, M., T. H. Pigford, and H. Levi, *Nuclear Chemical Engineering*, 2nd ed., McGraw-Hill, 1981.

[6] Kawasaki, D., J. Ahn, P. L. Chambré, and W. G. Halsey, Congruent Release of Long-Lived Radionuclides from Multiple Canister Arrays, *Nuclear Technology*, **148**, 181-193, 2004.

[7] J. E. Houseworth, S. Finsterle, and G. S. Bodvarsson, Flow and Transport in the Drift Shadow in a Dual-Continuum Model, *J. Cont. Hydrology*, **62-63**, 133-156, 2003.

[8] Japan Nuclear Cycle Development Institute, *Second Progress Report on Research and Development for the Geological Disposal of HLW in Japan, H12: Project to Establish the Scientific and Technical Basis for HLW Disposal in Japan*, JNC TN1400 99-021, 1999.

[9] Yamashita, T., et. al., High-Waste-Loading Vitrification Test of Radioactive HLLW, J20, *Proc. Atomic Energy Society of Japan*, Fall Meeting, JAERI, 1995.

[10] Sasage, K., et. al., Vitrification of Separated Components from HLLW, J34, *ibid*.

[11] Kawamura, K., *Mat. Res. Soc. Symp. Proc*., **353**, 1995.

[12] Tsuboya, T., *Enerugi-Shigen*, **13**(1), 1992.

[13] *PNC SN*8410 90-061, 1990

[14] Code of Federal Regulations, Title 10 Part 20.

Appendix: Input Data Files for ORIGEN2 Calculations

FBR Core Fuel

```
   -1
   -1
   -1
BAS        ORIGEN FOR MOX RECYCLE CORE
LIP    0 0 0
LIB    0 1 2 3 311 312 313 9 0 0 1 12
PHO    101 102 103 10
TIT    IRRADIATION
RDA    CORE    FUEL(FP)
INP    -1 1 -1 -1 1 1
MOV    -1 1 0 1.0
HED    1
BUP
IRP      510.0      815.50      1 2 4 2
IRP    1020.0      815.50      2 3 4 0
IRP    1530.0      815.50      3 4 4 0
IRP    2040.0      815.50      4 5 4 0
BUP
OPTL    8 8 8 8 8 8 8 8 8 18*8
OPTF    8 8 8 8 8 8 8 8 8 18*8
OPTA    8 8 8 8 8 8 8 8 8 18*8
OUT      5 1 -1 0
RDA      REFERENCE FOR CORE FUEL
MOV      5 1    0    1.0
TIT      DECAY
MOV      1    1    0    1.0
DEC             1.      1 2    1 2
DEC             1.      2 3    5 0
DEC             2.      3 4    5 0
DEC             4.      4 5    5 0
DEC             6.      5 6    5 0
DEC            50.      6 7    5 0
DEC           500.      7 8    5 0
OPTL    8 8 8 8 8 8 8 8 8 18*8
OPTF    8 8 8 8 1 8 1 8 1 18*8
OPTA    8 8 8 8 1 8 1 8 1 18*8
OUT      8 1 -1 0
STP    2
2 962450 0.0             922350 24.830+03 922360 0.0             922380 8254.20+03
2 932370 13.000+03 942380 28.610+03 942390 1407.21+03 942400 834.96+03
2 942410 111.84+03 942420 101.53+03 952410 52.010+03 952421 0.0
2 952430 26.010+03 962420 0.0             962430 0.0             962440 26.0100+03
3 601430 141.40+03            0 0.0
0
END
```

FBR Axial Blanket Fuel

```
   -1
   -1
```

```
   -1
BAS         ORIGEN FOR MOX RECYCLE CORE
LIP    0 0 0
LIB    0 1 2 3 314 315 316 9 0 0 1 13
PHO    101 102 103 10
TIT    IRRADIATION
RDA    AXIAL BLANKET(FP)
INP    -1 1 -1 -1 1 1
MOV    -1 1 0 1.0
HED    1
BUP
IRP      510.0        18.295    1 2 4 2
IRP     1020.0        18.295    2 3 4 0
IRP     1530.0        18.295    3 4 4 0
IRP     2040.0        18.295    4 5 4 0
BUP
OPTL    8 8 8 8 8 8 8 8 8 18*8
OPTF    8 8 8 8 8 8 8 8 8 18*8
OPTA    8 8 8 8 8 8 8 8 8 18*8
OUT      5 1 -1 0
RDA      REFERENCE FOR CORE FUEL
MOV      5 1    0    1.0
TIT      DECAY
MOV      1    1    0    1.0
DEC             1.      1 2    1 2
DEC             1.      2 3    5 0
DEC             2.      3 4    5 0
DEC             4.      4 5    5 0
DEC             6.      5 6    5 0
DEC            50.      6 7    5 0
DEC           500.      7 8    5 0
OPTL    8 8 8 8 8 8 8 8 8 18*8
OPTF    8 8 8 8 1 8 1 8 1 18*8
OPTA    8 8 8 8 1 8 1 8 1 18*8
OUT      8 1 -1 0
STP    2
2 922340 0.0             922350 28.000+03 922360 0.0             922380 9304.85+03
2           0 0.0
0
END
```

FBR Radial Blanket Fuel

```
   -1
   -1
   -1
BAS         ORIGEN FOR MOX RECYCLE CORE
LIP    0 0 0
LIB    0 1 2 3 317 318 319 9 0 0 1 14
PHO    101 102 103 10
TIT    IRRADIATION
RDA    RADIAL BLANKET(FP)
INP    -1 1 -1 -1 1 1
MOV    -1 1 0 1.0
HED    1
```

```
BUP
IRP     510.0         3.488    1 2 4 2
IRP    1020.0         3.488    2 3 4 0
IRP    1530.0         3.488    3 4 4 0
IRP    2040.0         3.488    4 5 4 0
BUP
OPTL    8 8 8 8 8 8 8 8 8 18*8
OPTF    8 8 8 8 8 8 8 8 8 18*8
OPTA    8 8 8 8 8 8 8 8 8 18*8
OUT     5 1 -1 0
RDA     REFERENCE FOR CORE FUEL
MOV      5 1    0    1.0
TIT     DECAY
MOV      1    1    0    1.0
DEC             1.      1 2    1 2
DEC             1.      2 3    5 0
DEC             2.      3 4    5 0
DEC             4.      4 5    5 0
DEC             6.      5 6    5 0
DEC            50.      6 7    5 0
DEC           500.      7 8    5 0
OPTL    8 8 8 8 8 8 8 8 8 8 8 8 8 8 8 8 8 8 8 8 8 8 8 8 8 8 8 8 8 8 8 8 8 8 8
OPTF    8 8 8 8 1 8 1 8 1 8 8 8 8 8 8 8 8 8 8 8 8 8 8 8 8 8 8 8 8 8 8 8 8 8 8
OPTA    8 8 8 8 1 8 1 8 1 8 8 8 8 8 8 8 8 8 8 8 8 8 8 8 8 8 8 8 8 8 8 8 8 8 8
OUT     8 1 -1 0
STP    2
2 922340 0.0             922350 27.080+03 922360 0.0             922380 9000.48+03
2          0 0.0
0
END
```

Appendix: FORTRAN Codes for Peak Mass of Nuclide in Environment

Congruent-Release Nuclides

(1) P vs. λ

```
      program peak_mass
      character axe*3
      double precision tlea,xn,arr1,ans,rsx,rlx,func
      common /par/ xn,tlea
      dimension arr1(101),ans(101)
      external func
C-------------------------------------------------------------
C  input parameter values
C-------------------------------------------------------------
      nnn = 101
        open(5,file='input.dat')
        open(8,file='out.dat')
      read(5,*) RSX,RLX,AXE   (Input minimum, maximum for λ, type of axis ("LOG" or "LIN"))
        n=100
        do 10 j=1,n
      read(5,*) xn, tlea      (Input Nx and T_L)
        if(xn.eq.9999.0.and.tlea.eq.9999.0) goto 100
C-------------------------------------------------------------------
C  set variable coordinates and fixed coordinates
C-------------------------------------------------------------------
C-------------------------------------------------------------------
C  output calculation conditions
C-------------------------------------------------------------------
      write(8,2001)
      write(8,2009) tlea
      write(8,2013) xn
 2001 format(/,5x,'(Parameter values)')
 2009 format(  5x,'normalized Leach time = ',1pe10.3)
 2013 format(  5x,'number of compartments in x = ', 1pe10.3)
C-------------------------------------------------------------------
C  one-variable case
C-------------------------------------------------------------------
C--Generate spatial grid points ----------------------------------
      call div(axe,rsx,rlx,arr1,nnn-1)
C--Calculate at each grid point ----------------------------------
      DO 8 I=1,nnn
      ANS(I)=func(ARR1(I))
    8 CONTINUE
C--output results ------------------------------------------------
      write(8,2031)
      do 9 i=1,nnn
        write(8,2032) arr1(i),ans(i)
    9 continue
   10 continue
 2031 format(10x,'lambda',10x,'P_value')
 2032 format(2(5x,1pe9.3))
  100 end
```

```
  SUBROUTINE DIV(AX,XMIN,XMAX,ARRAY,K)
  CHARACTER AX*3
  double precision xmin,xmax,array,del
  DIMENSION ARRAY(K+1)
  IF(AX.EQ.'LOG') THEN
    IF(XMIN.EQ.0.0d0) THEN
      XMIN=XMAX/10000.0d0
      DEL=10.0d0**(dlog10(XMAX/XMIN)/(dble(k)-1.0d0))
      array(1) = 0.0d0
      array(2) = xmin
      DO 1 J=3,k
      ARRAY(J)=ARRAY(J-1)*DEL
1     CONTINUE
      ARRAY(k+1)=XMAX
      RETURN
    ELSE
      DEL=10.0d0**(dlog10(XMAX/XMIN)/dble(k))
      ARRAY(1)=XMIN
      DO 2 J=2,k
2     ARRAY(J)=ARRAY(J-1)*DEL
      ARRAY(k+1)=XMAX
      RETURN
    END IF
  ELSE
    DEL=(XMAX-XMIN)/dble(k)
    ARRAY(1)=XMIN
    DO 3 J=2,k+1
    ARRAY(J)=ARRAY(J-1) + DEL
3   CONTINUE
    RETURN
  END IF
  END

  function func(xl)
  double precision tlea,xl,xn,func,tmp
  common /par/ xn,tlea
    if(xn.le.tlea) then
       if(1.0/xl.le.xn/2.0) then
          func=2.0/xl/xl/tlea/xn*exp(-2.0)
       else
          if(1.0/xl.le.(tlea-xn/2.0)) then
              func=1.0/xl/tlea*exp(-1.0-xl*xn/2.0)
          else
              tmp=sqrt(1.0+2.0*tlea*xn*xl*xl)-1.0
              func=tmp*exp(-xl*(tlea+xn)+tmp)/tlea/xn/xl/xl
          end if
       end if
    else
       if(1.0/xl.le.tlea/2.0) then
          func=2.0/xl/xl/tlea/xn*exp(-2.0)
       else
          if(1.0/xl.le.(xn-tlea/2.0)) then
              func=1.0/xl/xn*exp(-1.0-xl*tlea/2.0)
          else
                  tmp=sqrt(1.0+2.0*tlea*xn*xl*xl)-1.0
              func=tmp*exp(-xl*(tlea+xn)+tmp)/tlea/xn/xl/xl
            end if
```

```
   end if
    end if
return
end
```

Sample input data:

```
1.0e-5  1.0e2  "LOG"
1.0  100.0
3.0  100.0
9999.0  9999.0
```

Output for sample input:

```
(Parameter values)
normalized Leach time =  1.000E+02
number of compartments in x =  1.000E+00
    lambda        P_value
1.000E-05    9.990E-01
1.175E-05    9.988E-01
1.380E-05    9.986E-01
1.622E-05    9.984E-01
1.905E-05    9.981E-01
2.239E-05    9.977E-01
2.630E-05    9.973E-01
3.090E-05    9.969E-01
3.631E-05    9.963E-01
4.266E-05    9.957E-01
5.012E-05    9.950E-01

   (omit)

1.698E+01    9.385E-06
1.995E+01    6.799E-06
2.344E+01    4.925E-06
2.754E+01    3.568E-06
3.236E+01    2.585E-06
3.802E+01    1.873E-06
4.467E+01    1.357E-06
5.248E+01    9.827E-07
6.166E+01    7.119E-07
7.244E+01    5.158E-07
8.511E+01    3.736E-07
1.000E+02    2.707E-07

(Parameter values)
normalized Leach time =  1.000E+02
number of compartments in x =  3.000E+00
    lambda        P_value
1.000E-05    9.990E-01
1.175E-05    9.988E-01
1.380E-05    9.986E-01
1.622E-05    9.983E-01
1.905E-05    9.980E-01
2.239E-05    9.977E-01
2.630E-05    9.973E-01
```

```
    3.090E-05    9.968E-01

       (omit)

    1.995E+01    2.266E-06
    2.344E+01    1.642E-06
    2.754E+01    1.189E-06
    3.236E+01    8.616E-07
    3.802E+01    6.242E-07
    4.467E+01    4.522E-07
    5.248E+01    3.276E-07
    6.166E+01    2.373E-07
    7.244E+01    1.719E-07
    8.511E+01    1.245E-07
    1.000E+02    9.022E-08
```

(2) P vs. N_x

```
      program peak_mass
      character axe*3
      double precision tlea,xn,arr1,ans,rsx,rlx,func,xl
      common /par/ xl,tlea
      dimension arr1(31),ans(31)
      external func
C-------------------------------------------------------------
C  input parameter values
C-------------------------------------------------------------
      nnn = 31
      open(5,file='input.dat')
        open(8,file='out.dat')
      read(5,*) RSX,RLX,AXE
        n=30
        do 10 j=1,n
      read(5,*) xl, tlea
        if(xl.eq.9999.0.and.tlea.eq.9999.0) goto 100
C--------------------------------------------------------------------
C  set variable coordinates and fixed coordinates
C--------------------------------------------------------------------
C--------------------------------------------------------------------
C  output calculation conditions
C--------------------------------------------------------------------
      write(8,2001)
      write(8,2009) tlea
      write(8,2013) xl
 2001 format(/,5x,'(Parameter values)')
 2009 format(  5x,'normalized Leach time = ',1pe10.3)
 2013 format(  5x,'normalized lambda = ', 1pe10.3)
C--------------------------------------------------------------------
C  one-variable case
C--------------------------------------------------------------------
C--Generate spatial grid points ------------------------------------
      call div(axe,rsx,rlx,arr1,nnn-1)
C--Calculate at each grid point ------------------------------------
      DO 8 I=1,nnn
      ANS(I)=func(ARR1(I))
    8 CONTINUE
C--output results --------------------------------------------------
```

```
    write(8,2031)
    do 9 i=1,nnn
      write(8,2032) arr1(i),ans(i)
   9 continue
  10 continue
2031 format(10x,'Nx',10x,'P_value')
2032 format(2(5x,1pe9.3))
 100 end

    SUBROUTINE DIV(AX,XMIN,XMAX,ARRAY,K)
      (same as in the previous program)

    function func(xn)
    double precision tlea,xl,xn,func,tmp
    common /par/ xl,tlea
      if(xn.le.tlea) then
        if(1.0/xl.le.xn/2.0) then
          func=2.0/xl/xl/tlea/xn*exp(-2.0)
        else
          if(1.0/xl.le.(tlea-xn/2.0)) then
              func=1.0/xl/tlea*exp(-1.0-xl*xn/2.0)
          else
              tmp=sqrt(1.0+2.0*tlea*xn*xl*xl)-1.0
              func=tmp*exp(-xl*(tlea+xn)+tmp)/tlea/xn/xl/xl
          end if
        end if
      else
        if(1.0/xl.le.tlea/2.0) then
          func=2.0/xl/xl/tlea/xn*exp(-2.0)
        else
          if(1.0/xl.le.(xn-tlea/2.0)) then
              func=1.0/xl/xn*exp(-1.0-xl*tlea/2.0)
          else
                  tmp=sqrt(1.0+2.0*tlea*xn*xl*xl)-1.0
              func=tmp*exp(-xl*(tlea+xn)+tmp)/tlea/xn/xl/xl
            end if
       end if
        end if
    return
    end
```

Solubility-Limited Nuclide

(1) P vs. σ

```
      program normalized_mass_Sol_Lim_Peak
      character axe*3
      double precision P, beta, zeta, xl, xn, xmu, gamma, sigma, cnx
      double precision xkappa, alpha, Tnx, qbar, ptnx, tpeak, pnx
      double precision xmw, Tdep, arr1, rsx, rlx, pp1, cnxnx
      common /par/sigma, beta, zeta, xl, xn, xmu, cnx, Tnx, Tdep
      dimension arr1(101)
      external xmw
      open(5,file='input_peak.dat')
      open(8,file='out_peak.dat')
```

```
      read(5,*) xn, xl, alpha, xmu        (Input Nx, λ, α, μ)
      read(5,*) RSX,RLX,AXE               (Ranges of 1/σ)
      write(8,2001)
      write(8,2013) xn
      write(8,2014) xl
      write(8,2015) alpha
      write(8,2016) xmu
      xkappa=sqrt(xl/alpha)
      beta=alpha*xkappa/sinh(xkappa)
      zeta=xl+beta*xmu*cosh(xkappa)
      gamma=1.0/(1.0+zeta)
      cnx=xmu*beta/zeta*(1.0-gamma**xn)
      write(8,2018) xkappa
      write(8,2019) beta
      write(8,2020) zeta
      write(8,2021) gamma
      write(8,2022) cnx
 2001 format(/,5x,'(Parameter values)')
 2013 format(  5x,'number of compartments in x = ', 1pe10.3)
 2014 format(  5x,'normalized decay const, lambda = ', 1pe10.3)
 2015 format(  5x,'Fourier number, alpha = ', 1pe10.3)
 2016 format(  5x,'ratio of buffer to rock capacity, mu = ',1pe10.3)
 2018 format(  5x,'kappa = ', 1pe10.3)
 2019 format(  5x,'beta = ',1pe10.3)
 2020 format(  5x,'zeta = ',1pe10.3)
 2021 format(  5x,'gamma = ',1pe10.3)
 2022 format(  5x,'cnx = ',1pe10.3)
C--Generate grid points -----------------------------------
     nnn = 101
     call div(axe,rsx,rlx,arr1,nnn-1)
     write(8,2031)
 2031 format(5x,'sigma^-1',10x,'P_peak',10x,'tpeak',10x,'qbar',10x,'Tnx',
    +      10x,'Tdep')
C--Calculate at each grid point ---------------------------------
     DO 8 I=1,nnn
       sigma=arr1(i)
       qbar=beta*sigma*(cosh(xkappa)-cnx)
       Tnx=xn+1.0/xl*log(1.0+xl*xmw(xn)/qbar)
     Call NR(Tdep)
       if(xn.le.Tdep) then
         ptnx=P(Tnx)
         tpeak=Tnx+1.0/xl+xn-sqrt((xn+1.0/xl)**2-2.0*xn/xl
    +           +2.0*xmu*xn*xn/sigma/cnx*ptnx)
       pp1=P(tpeak)
       else
         cnxnx=xmu*beta/zeta*(1.0-exp(-zeta*Tdep))*exp(-xl*(xn-Tdep))
         pnx=P(xn)
         tpeak=xn+Tdep+1.0/xl-sqrt((Tdep+1.0/xl)**2
    +      -2.0*Tdep/xl+2.0*Tdep*pnx/(sigma*cnxnx/xmu/xn))
         pp1=P(tpeak)
       end if
     write(8,2032) 1.0/sigma,pp1,tpeak,qbar,Tnx,Tdep
   8 CONTINUE
 2032 format(6(5x,1pe10.2))
     end
```

```
SUBROUTINE DIV(AX,XMIN,XMAX,ARRAY,K)
  (Same as the previous code)

  function P(t)
  double precision P, t, sigma, beta, zeta, xl, xn
  double precision xmu, cnx, Tnx, Tdep
  double precision P1, P2, P3, P4, P5, P6, P7
  common /par/sigma, beta, zeta, xl, xn, xmu, cnx, Tnx, Tdep
  if(xn.le.Tdep) then
    if(t.le.xn) then
               P=P1(t)
           else
             if(t.le.Tnx) then
                  P=P2(t)
             else
                  if(t.le.(Tnx+xn)) then
                  P=P3(t)
          else
          P=P4(t)
        end if
       end if
    end if
  else if(t.le.Tdep) then
                  P=P1(t)
           else
             if(t.le.xn) then
                  P=P5(t)
           else
             if(t.le.(xn+Tdep)) then
                  P=P6(t)
             else
                  P=P7(t)
        end if
       end if
  end if
  return
  end

  function P1(t)
  double precision P1, t, sigma, beta, zeta, xl
  double precision xn, xmu, cnx, Tnx, Tdep
  common /par/sigma, beta, zeta, xl, xn, xmu, cnx, Tnx, Tdep
  P1=sigma*beta/zeta/xn*((1.0-exp(-xl*t))
  +        /xl-(exp(-zeta*t)-exp(-xl*t))/(xl-zeta))
  return
  end

  function P2(t)
  double precision P2, P1,t, sigma, beta, zeta
  double precision xl, xn, xmu, cnx, Tnx, Tdep
  common /par/sigma, beta, zeta, xl, xn, xmu, cnx, Tnx, Tdep
  external P1
  P2=P1(xn)*exp(-xl*(t-xn))
  P2=P2+sigma*cnx/xmu/xl/xn*(1.0-exp(-xl*(t-xn)))
  return
  end
```

```
      function P3(t)
      double precision P2, P3,t, sigma, beta, zeta
      double precision xl, xn, xmu, cnx, Tnx, Tdep
      common /par/sigma, beta, zeta, xl, xn, xmu, cnx, Tnx, Tdep
      external P2
      P3=P2(Tnx)*exp(-xl*(t-Tnx))
      P3=P3+sigma*cnx/xmu/xn*((t-Tnx)-(t-Tnx)**2/2.0/xn)
     +     *exp(-xl*(t-Tnx))
      return
      end

      function P4(t)
      double precision P4, P3, t, sigma, beta, zeta
      double precision xl, xn, xmu, cnx, Tnx, Tdep
      common /par/sigma, beta, zeta, xl, xn, xmu, cnx, Tnx, Tdep
      external P3
      P4=P3(Tnx+xn)*exp(-xl*(t-Tnx-xn))
      return
      end

      function P5(t)
      double precision P5, P1,t, sigma, beta, zeta
      double precision xl, xn, xmu, cnx, Tnx, Tdep
      double precision cnxt
      common /par/sigma, beta, zeta, xl, xn, xmu, cnx, Tnx, Tdep
      external P1
      cnxt=xmu*beta/zeta*(1.0-exp(-zeta*Tdep))
      P5=P1(Tdep)*exp(-xl*(t-Tdep))
      P5=P5+sigma*cnxt/xmu/xn*(t-Tdep)*exp(-xl*(t-Tdep))
      return
      end

      function P6(t)
      double precision P6, P5,t, sigma, beta, zeta
      double precision xl, xn, xmu, cnx, Tnx, Tdep
      double precision cnxnx
      common /par/sigma, beta, zeta, xl, xn, xmu, cnx, Tnx, Tdep
      external P5
      cnxnx=xmu*beta/zeta*(1.0-exp(-zeta*Tdep))*exp(-xl*(xn-Tdep))
      P6=P5(xn)+sigma*cnxnx/xmu/xn*(t-xn-(t-xn)**2/2.0/Tdep)
      P6=P6*exp(-xl*(t-xn))
      return
      end

      function P7(t)
      double precision P7, P6,t, sigma, beta, zeta
      double precision xl, xn, xmu, cnx, Tnx, Tdep
      common /par/sigma, beta, zeta, xl, xn, xmu, cnx, Tnx, Tdep
      external P6
      P7=P6(Tdep+xn)*exp(-xl*(t-xn-Tdep))
      return
      end

     Subroutine NR(ans)
     Integer JMAX
     double precision ans,xacc, xmw, xmwd, dx
     external xmw, xmwd
```

```
      Parameter (JMAX=100)      !Set to maximum number of iterations.
      Parameter (xacc=1.0e-3)
!       Using the Newton-Raphson method.
      Integer j
      ans=0.0        !Initial guess.
      do j=1,JMAX
        dx=xmw(ans)/xmwd(ans)
          ans=ans-dx
        if(abs(dx).lt.xacc) return    !Convergence.
      end do
      pause 'NR exceeded maximum iterations'
      end

        function xmw(t)
        double precision xmw, t, sigma, beta, zeta, xl, xn, xmu
        double precision cnx, Tnx, Tdep
      common /par/sigma, beta, zeta, xl, xn, xmu, cnx, Tnx, Tdep
        xmw=exp(-xl*t)+beta*sigma/xl*(xmu*beta/zeta-cosh(xkappa))
     +     *(1.0-exp(-xl*t))+sigma*beta/zeta*(exp(-zeta*t)-
     +     exp(-xl*t))/cosh(xkappa)
        return
        end

        function xmwd(t)
        double precision xmwd, t, sigma, beta, zeta, xl, xn, xmu
        double precision cnx, Tnx, Tdep
      common /par/sigma, beta, zeta, xl, xn, xmu, cnx, Tnx, Tdep
        xmwd=-xl*exp(-xl*t)+beta*sigma*(xmu*beta/zeta-cosh(xkappa))
     +     *exp(-xl*t)+sigma*beta/zeta/cosh(xkappa)
     +     *(xl*exp(-xl*t)-zeta*exp(-zeta*t))
        return
        end
```

(2) P vs. N_x

```
      program normalized_mass_Sol_Lim_Peak
        character axe*3
      double precision P, beta, zeta, xl, xn, xmu, gamma, sigma, cnx
        double precision xkappa, alpha, Tnx, qbar, ptnx, tpeak, pnx
        double precision xmw, Tdep, arr1, rsx, rlx, pp1, cnxnx
        common /par/sigma, beta, zeta, xl, xn, xmu, cnx, Tnx, Tdep
      dimension arr1(31)
        external xmw
        open(5,file='input_peak_nx.dat')
        open(8,file='out_peak.dat')
        read(5,*) sigma, xl, alpha, xmu
      read(5,*) RSX,RLX,AXE
        write(8,2001)
      write(8,2013) sigma
        write(8,2014) xl
        write(8,2015) alpha
        write(8,2016) xmu
      xkappa=sqrt(xl/alpha)
        beta=alpha*xkappa/sinh(xkappa)
        zeta=xl+beta*xmu*cosh(xkappa)
        gamma=1.0/(1.0+zeta)
        write(8,2018) xkappa
```

```
       write(8,2019) beta
       write(8,2020) zeta
       write(8,2021) gamma
 2001 format(/,5x,'(Parameter values)')
 2013 format(  5x,'sigma = ', 1pe10.3)
 2014 format(  5x,'normalized decay const, lambda = ', 1pe10.3)
 2015 format(  5x,'Fourier number, alpha = ', 1pe10.3)
 2016 format(  5x,'ratio of buffer to rock capacity, mu = ',1pe10.3)
 2018 format(  5x,'kappa = ', 1pe10.3)
 2019 format(  5x,'beta = ',1pe10.3)
 2020 format(  5x,'zeta = ',1pe10.3)
 2021 format(  5x,'gamma = ',1pe10.3)
C--Generate grid points -----------------------------------
     nnn = 31
     call div(axe,rsx,rlx,arr1,nnn-1)
     write(8,2031)
 2031 format(5x,'xn',10x,'P_peak',10x, 'Tdep')
C--Calculate at each grid point ---------------------------------
     DO 8 I=1,nnn
       xn=arr1(i)
       cnx=xmu*beta/zeta*(1.0-gamma**xn)
       qbar=beta*sigma*(cosh(xkappa)-cnx)
       Tnx=xn+1.0/xl*log(1.0+xl*xmw(xn)/qbar)
     Call NR(Tdep)
       if(xn.le.Tdep) then
         ptnx=P(Tnx)
         tpeak=Tnx+1.0/xl+xn-sqrt((xn+1.0/xl)**2-2.0*xn/xl
    +            +2.0*xmu*xn*xn/sigma/cnx*ptnx)
       pp1=P(tpeak)
       else
         cnxnx=xmu*beta/zeta*(1.0-exp(-zeta*Tdep))*exp(-xl*(xn-Tdep))
         pnx=P(xn)
         tpeak=xn+Tdep+1.0/xl-sqrt((Tdep+1.0/xl)**2
    +      -2.0*Tdep/xl+2.0*Tdep*pnx/(sigma*cnxnx/xmu/xn))
         pp1=P(tpeak)
       end if
     write(8,2032) xn,pp1,Tdep
   8 CONTINUE
 2032 format(3(5x,1pe10.2))
     end

     SUBROUTINE DIV(AX,XMIN,XMAX,ARRAY,K)
       (Same as previous)

       function P(t)
       (same as previous)

       function P1(t)
       (same as previous)

       function P2(t)
       (same as previous)

       function P3(t)
       (same as previous)

       function P4(t)
```

```
  (same as previous)

  function P5(t)
  (same as previous)

  function P6(t)
  (same as previous)

  function P7(t)
  (same as previous)

Subroutine NR(ans)
  (same as previous)

  function xmw(t)
  (same as previous)

  function xmwd(t)
  (same as previous)
```